

Lagrangian torus fibrations
(notes in progress)

Jonny Evans

February 8, 2019

Contents

| | | |
|----------|---|-----------|
| 1 | Introduction | 5 |
| 2 | The Arnol'd-Liouville theorem | 7 |
| 2.1 | Hamilton's equations in 2D | 7 |
| 2.2 | Symplectic geometry | 9 |
| 2.3 | Integrable Hamiltonian systems | 11 |
| 2.4 | Liouville coordinates | 13 |
| 2.5 | The Arnol'd-Liouville theorem | 15 |
| 2.6 | Exercises | 18 |
| 3 | Hamiltonian torus actions | 21 |
| 3.1 | Global action-angle coordinates | 21 |
| 3.2 | Hamiltonian group actions | 22 |
| 3.3 | Examples | 27 |
| 3.4 | Visible Lagrangian submanifolds | 32 |
| 3.5 | Exercises | 36 |
| 4 | Focus-focus singularities | 41 |
| 4.1 | Flux map | 41 |
| 4.2 | Focus-focus singularities | 44 |
| 4.3 | Action coordinates | 47 |
| 4.4 | Model neighbourhoods | 52 |
| 4.5 | The Auroux system | 53 |

| | | |
|----------|---|-----------|
| 4.6 | Symington's theorem | 58 |
| 4.7 | Exercises | 59 |
| 5 | Almost toric manifolds | 63 |
| 5.1 | Lagrangian torus fibrations | 63 |
| 5.2 | Operations | 64 |
| 5.3 | Examples | 74 |
| 5.4 | Exercises | 82 |
| 6 | Ruan's construction | 85 |
| 6.1 | Symplectic parallel transport | 85 |
| 6.2 | Lagrangian torus fibrations | 88 |
| 6.3 | Quartic pencil | 91 |
| 6.4 | Exercises | 96 |
| 7 | Solutions to selected exercises | 97 |
| 7.1 | Chapter 1 | 97 |
| 7.2 | Chapter 5 | 99 |

Chapter 1

Introduction

Chapter 2

The Arnol'd-Liouville theorem

2.1 Hamilton's equations in 2D

The simplest nontrivial case of Hamilton's equations is

$$\dot{p} = -\frac{\partial H}{\partial q}, \quad \dot{q} = \frac{\partial H}{\partial p}. \quad (2.1)$$

where $(p(t), q(t))$ is a path in the plane and $H(p, q)$ is a function of p and q . Physically, we could think of q as being position, p as being momentum and H as being energy¹. Observe that

$$\dot{H} = \frac{\partial H}{\partial p} \dot{p} + \frac{\partial H}{\partial q} \dot{q} = \dot{q} \dot{p} - \dot{p} \dot{q} = 0,$$

¹If $H = \frac{p^2}{2m}$ (the usual expression for kinetic energy) then Hamilton's equations give the usual expression $p = m\dot{q}$ for momentum.

so energy is conserved.

Equation (2.1) is a machine for turning a function $H(p, q)$ (the *Hamiltonian*) into a one-parameter family of diffeomorphisms

$$\phi_t^H(p(0), q(0)) = (p(t), q(t))$$

(the *Hamiltonian flow*). The flow satisfies $H(\phi_t^H(p, q)) = H(p, q)$.

Example 2.1.1. If $H = \frac{1}{2}(p^2 + q^2)$ then $\dot{p} = -q$, $\dot{q} = p$, so $\begin{pmatrix} p(t) \\ q(t) \end{pmatrix} = \begin{pmatrix} \cos t & -\sin t \\ \sin t & \cos t \end{pmatrix} \begin{pmatrix} p(0) \\ q(0) \end{pmatrix}$. This corresponds to a rotation of the plane with constant angular speed.

Example 2.1.2. If $H = \sqrt{p^2 + q^2}$ then $\dot{p} = -q/H$, $\dot{q} = p/H$, and since $\dot{H} = 0$ the solution is

$$\begin{pmatrix} p(t) \\ q(t) \end{pmatrix} = \begin{pmatrix} \cos(t/H) & -\sin(t/H) \\ \sin(t/H) & \cos(t/H) \end{pmatrix} \begin{pmatrix} p(0) \\ q(0) \end{pmatrix}.$$

This flow has the same orbits (circles of radius H), but now the orbit at radius H has period $2\pi H$.

Theorem 2.1.3. *If all level sets of H are circles, there exists a diffeomorphism $f: \mathbf{R} \rightarrow \mathbf{R}$ such that for the Hamiltonian $f \circ H$ all orbits have period 2π .*

Proof. Using $f \circ H$, we have $\dot{p} = -\frac{\partial(f \circ H)}{\partial q} = -f'(H)\frac{\partial H}{\partial q}$ and $\dot{q} = \frac{\partial(f \circ H)}{\partial p} = f'(H)\frac{\partial H}{\partial p}$, so the effect of postcomposing H with f is to rescale (\dot{p}, \dot{q}) by $f'(H)$ (which is constant along orbits). If the period of the orbit $O_b := H^{-1}(b)$ is $T(b)$ then the new period of O_b with Hamiltonian $f \circ H$ is therefore $T(b)/f'(b)$. If we use $f(b) = \frac{1}{2\pi} \int_0^b T(c)dc$ then the new periods are all equal to 2π . \square

Periods are usually hard to find explicitly; for example, elliptic functions were invented to describe periods in Keplerian planetary motion. Similarly, the map f is difficult to write down explicitly in examples.

Theorem 2.1.4. *In a 1-parameter family of closed orbits O_b , $b \in \mathbf{R}$, of a Hamiltonian system, the period of O_b is $\frac{d}{db} \int_{O_b} pdq$.*

Remark 2.1.5. This means that $f(b) = \frac{1}{2\pi} \int_{O_b} pdq$ is another way of writing the function we found in Theorem 2.1.3).

Proof. Assume for simplicity² that we have coordinates (p, q) , with $q \in \mathbf{R}/2\pi\mathbf{Z}$, such that the orbits have the form $O_b := \{(p_b(q), q) : q \in \mathbf{R}/2\pi\mathbf{Z}\}$ for some functions p_b . Then

$$\begin{aligned} T(b) &= \int_0^{2\pi} \frac{dt}{dq} dq = \int_0^{2\pi} \frac{dq}{\dot{q}} \\ &= \int_0^{2\pi} \frac{dq}{\partial H / \partial p_b} = \int_0^{2\pi} \frac{\partial p_b}{\partial H} dq = \frac{d}{db} \int_0^{2\pi} pdq. \quad \square \end{aligned}$$

Our goal in this first lecture is to generalise these observations to Hamiltonian systems in higher dimensions. It will be convenient to introduce the language of symplectic geometry.

2.2 Symplectic geometry

Definition 2.2.1. Let X be a manifold and ω a 2-form. Define a map³ $\flat: \Gamma(TX) \rightarrow \Gamma(T^*X)$ by $\flat(V) = \iota_V \omega$. We say that ω is *nondegenerate* if \flat is an isomorphism, in which case we write \sharp for its inverse. A *symplectic form* is a closed, nondegenerate 2-form.

Definition 2.2.2. Given a smooth function $H: X \rightarrow \mathbf{R}$ and a symplectic form ω on X , we get a vector field $V_H := -\sharp(dH)$ (i.e. $\iota_{V_H} \omega = -dH$). We call such vector fields *Hamiltonian*. The flow ϕ_t^H along V_H is called a *Hamiltonian flow*.

²One can always find coordinates (p, q) in which the orbits have this form.

³ $\Gamma(TX)$ denotes the space of vector fields and $\Gamma(T^*X)$ the space of 1-forms.

Example 2.2.3. Let $\omega = dp \wedge dq$ on $X = \mathbf{R}^2$. Then, if $(p(t), q(t)) = \phi_t^H(p(0), q(0))$, we have $V_H = (\dot{p}, \dot{q})$ and $\iota_{V_H}\omega = \dot{p}dq - \dot{q}dp = -\frac{\partial H}{\partial p}dp - \frac{\partial H}{\partial q}dq$ so we recover Hamilton's equations (2.1).

Lemma 2.2.4. *A Hamiltonian flow ϕ_t^H satisfies $(\phi_t^H)^*\omega = \omega$ and $(\phi_t^H)^*H = H$.*

Proof. We first show that the Lie derivatives $L_{V_H}\omega$ and $L_{V_H}H$ vanish. For this, we use Cartan's formula $L_V\eta = \iota_V d\eta + d\iota_V\eta$ for the Lie derivative of a differential form η along a vector field V . We have

$$L_{V_H}\omega = d\iota_{V_H}\omega + \iota_{V_H}d\omega = -ddH = 0,$$

as $d\omega = 0$ and $\iota_{V_H}\omega = -dH$, and

$$L_{V_H}H = \iota_{V_H}dH = -\omega(V_H, V_H) = 0,$$

as ω is antisymmetric.

Now note that $\frac{d}{dt}(\phi_t^H)^*\omega = (\phi_t^H)^*L_{(\phi_t^H)^*V_H}\omega$ and $(\phi_t^H)^*V_H = V_H$, so $L_{V_H}\omega = 0$ implies $\frac{d}{dt}(\phi_t^H)^*\omega = 0$, so $(\phi_t^H)^*\omega = \omega$. Similarly, the fact that $(\phi_t^H)^*H = H$ follows from the vanishing of $L_{V_H}H$. \square

Remark 2.2.5. Note that if H is also allowed to depend explicitly on t (a *non-autonomous Hamiltonian flow*) then the previous argument for conservation of energy breaks down. Nonetheless, the flow preserves the symplectic form.

Lemma 2.2.6. *The Lie bracket of two Hamiltonian vector fields V_F and V_G is the Hamiltonian vector field $V_{\{F,G\}}$, where $\{F,G\} = \omega(V_F, V_G)$.*

Proof. We have $\iota_{[V_F, V_G]}\omega = [L_{V_F}, \iota_{V_G}]\omega$. Since V_F is symplectic, the term $\iota_{V_G}L_{V_F}\omega$ vanishes. Expanding the remaining term using Cartan's formula, and remembering that $d\iota_{V_G}\omega = -ddG = 0$, we get $\iota_{[V_F, V_G]}\omega = d\iota_{V_F}\iota_{V_G}\omega$. Since $\iota_{V_F}\iota_{V_G}\omega = -\omega(V_F, V_G)$ this tells us that $[V_F, V_G] = V_{\omega(V_F, V_G)}$ as required. \square

Definition 2.2.7. The quantity $\{F, G\}$ is called the *Poisson bracket* of F and G . We say that F and G *Poisson commute* if $\{F, G\} = 0$.

Lemma 2.2.8 (Exercise). *If F and G are smooth functions and we define $F_t(x) := F(\phi_t^G(x))$ then $\dot{F}_t = \{G, F_t\}$.*

2.3 Integrable Hamiltonian systems

Suppose we have a symplectic manifold (X, ω) and a map $H = (H_1, \dots, H_n): X \rightarrow \mathbf{R}^n$ for which the components H_1, \dots, H_n satisfy $\{H_i, H_j\} = 0$ for all pairs i, j . In what follows, we will assume that the vector fields V_{H_i} can be integrated for all time, so that the flows $\phi_t^{H_i}$ are defined for all $t \in \mathbf{R}$. The flows $\phi_{t_1}^{H_1}, \dots, \phi_{t_n}^{H_n}$ commute with one another and hence define an action of the group \mathbf{R}^n on X . We call this a *Hamiltonian \mathbf{R}^n -action*.

Example 2.3.1. Consider the \mathbf{R}^2 -action on \mathbf{R}^2 where (s, t) acts by $(s, t) \cdot (x_0, y_0) = (x_0 + s, y_0 + t) = \phi_t^x \phi_s^y(x_0, y_0)$. Even though ϕ_t^x and ϕ_s^y define Hamiltonian \mathbf{R} -actions which commute, this example is *not* a Hamiltonian \mathbf{R}^2 -action because the Poisson bracket $\{x, y\} = 1$ is not zero (i.e. they do not *Poisson-commute*).

More generally, for a Lie group G with Lie algebra \mathfrak{g} , a Hamiltonian G -action is a G -action in which every one-parameter subgroup $\exp(t\xi)$ acts as a Hamiltonian flow $\phi_t^{H_\xi}$, and the assignment $\xi \mapsto H_\xi$ is a Lie algebra map (i.e. $H_{[\xi_1, \xi_2]} = \{H_{\xi_1}, H_{\xi_2}\}$).

Definition 2.3.2. A submanifold L of a symplectic manifold (X, ω) is called *isotropic* if ω vanishes on vectors tangent to L . If $\dim X = 2n$ then $\dim L \leq n$ for an isotropic submanifold L (exercise) and we say that L is *Lagrangian* if L is isotropic and $\dim L = n$.

Lemma 2.3.3. *The orbits of a Hamiltonian \mathbf{R}^n -action on a symplectic manifold (X, ω) are isotropic. As a consequence, if X con-*

tains a regular point⁴ of H then $n \leq \frac{1}{2} \dim X$.

Proof. The tangent space to an orbit is spanned by the vectors V_{H_1}, \dots, V_{H_n} , which satisfy $\omega(V_{H_i}, V_{H_j}) = \{H_i, H_j\} = 0$, so the orbits are isotropic. If $x \in X$ is a regular point then the differentials dH_1, \dots, dH_n are linearly independent at x , so the vectors $V_{H_1}(x), \dots, V_{H_n}(x)$ span an n -dimensional isotropic space, which can have dimension at most $\dim X/2$. \square

Corollary 2.3.4. *If $\dim X = 2n$ and $H: X \rightarrow \mathbf{R}^n$ is a smooth map with connected fibres whose components satisfy $\{H_i, H_j\} = 0$, then the regular fibres are Lagrangian orbits of the \mathbf{R}^n -action.*

Proof. Since $\{H_i, H_j\} = 0$, Lemma 2.2.8 implies that H_j is constant along the flow of V_{H_i} . In particular, this means that if $x \in H^{-1}(y)$ then $\text{Orb}(x) \subset H^{-1}(y)$. Now let y be a regular value with fibre $H^{-1}(y)$. The fibre is n -dimensional, and the orbit of each point in the fibre is an open n -dimensional isotropic (i.e. Lagrangian) submanifold, so the fibre is a union of open submanifolds. If the fibre is connected then it cannot be a union of more than one open submanifold, so the \mathbf{R}^n -action is transitive on connected regular fibres, as required. \square

Definition 2.3.5. Let (X, ω) be a $2n$ -dimensional symplectic manifold. We say that a smooth map $H: X \rightarrow \mathbf{R}^n$ is a *complete commuting Hamiltonian system* if the components H_1, \dots, H_n satisfy $\{H_i, H_j\} = 0$ for all i, j . We say that a complete commuting Hamiltonian system H is an *integrable Hamiltonian system* if

- $H(X)$ contains a dense open set of regular values,

⁴Recall if $H: X \rightarrow Y$ is a smooth map then a point $x \in X$ is called *regular* if dH is surjective at x and a point $y \in \mathbf{R}^n$ is called a *regular value* if the fibre $H^{-1}(y)$ consists entirely of regular points; in this case we call $H^{-1}(y)$ a *regular fibre*.

- H is proper (preimages of compact sets are compact) and has connected fibres.

The first assumption rules out trivial examples; the properness condition ensures that the flows of the vector fields V_{H_1}, \dots, V_{H_n} exist for all time.

We write $\Phi_t^H := \phi_{t_1}^{H_1} \dots \phi_{t_n}^{H_n}$ for this \mathbf{R}^n -action and $Orb(x)$ for its orbit through $x \in X$. Each orbit is isotropic and the orbit of a regular point is Lagrangian.

2.4 Liouville coordinates

Definition 2.4.1. A local Lagrangian section of an integrable Hamiltonian system $H: X \rightarrow \mathbf{R}^n$ is a Lagrangian embedding $\sigma: U \rightarrow X$ where $U \subset H(X)$ is an open set and $H \circ \sigma(b) = b$ for all $b \in U$.

Lemma 2.4.2 (Exercise). *There always exists a local Lagrangian section through any regular point x .*

Theorem 2.4.3 (Liouville coordinates). *Let $H: X \rightarrow \mathbf{R}^n$ be an integrable Hamiltonian system and $\sigma: U \rightarrow X$ be a local Lagrangian section. Define*

$$\Psi: U \times \mathbf{R}^n \rightarrow X, \quad \Psi(b, t) = \Phi_t^H(\sigma(b)).$$

Then Ψ is both an immersion and a submersion and $\Psi^\omega = \sum db_i \wedge dt_i$, where (b_1, \dots, b_n) are the standard coordinates on $U \subset \mathbf{R}^n$. This means that $(b_1, \dots, b_n, t_1, \dots, t_n)$ provide local symplectic coordinates on a neighbourhood of $\sigma(U)$; we call these Liouville coordinates.*

Proof. • $\Psi_*\partial_{b_i}$ and $\Psi_*\partial_{b_j}$ are tangent to $\Phi_t^H(\sigma(U))$, which is the image of a Lagrangian under a series of Hamiltonian flows, hence Lagrangian. Therefore $\omega(\Psi_*\partial_{b_i}, \Psi_*\partial_{b_j}) = 0$.

- $\Psi_*\partial_{t_i} = V_{H_i}$, so

$$\omega(\Psi_*\partial_{t_i}, \Psi_*\partial_{t_j}) = \omega(V_{H_i}, V_{H_j}) = \{H_i, H_j\} = 0.$$

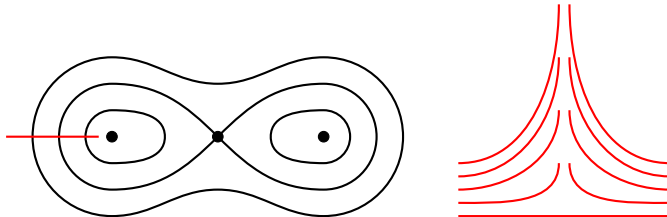
- $\omega(\Psi_*\partial_{b_i}, \Psi_*\partial_{t_j}) = dH_j(\Psi_*\partial_{b_i})$, and, since $(H_j \circ \Psi)(b, t) = b_j$ (as the flow along Ψ_t preserves the level sets of H_j) we have $dH_j(\Psi_*(\partial_{b_i})) = db_j(\partial_{b_i}) = \delta_{ij}$. Therefore $\Psi^*\omega = \sum_{i=1}^n db_i \wedge dt_i = \omega_0$.

Note that this implies that Ψ is both an immersion and a submersion (if it failed to be an immersion or a submersion at some point then $\Psi^*\omega$ would be degenerate there). \square

Definition 2.4.4. We call the subset $\Lambda := \Psi^{-1}(\sigma(U)) \subset U \times \mathbf{R}^n$ the *period lattice*. It is a Lagrangian submanifold with respect to $\sum db_i \wedge dt_i$ since Ψ is a local symplectomorphism and $\sigma(U)$ is Lagrangian. We say that the period lattice is *standard* if it is equal to $U \times (2\pi\mathbf{Z})^n$.

Example 2.4.5. The period lattice in Example 2.1.1 is standard, while in Example 2.1.2 it is $\{(r, 2\pi r) : r > 0\}$, where $U = \mathbf{R}_{>0}$ is the set of positive radii and $\sigma(r) = r$.

Example 2.4.6. Consider the Hamiltonian system on \mathbf{R}^2 whose level sets are shown in the figure below. This Hamiltonian generates an \mathbf{R} -action whose orbits are: the fixed points; the two separatrices; the closed loops. The separatrices have infinite period (it takes infinitely long to flow around them). If we take as Lagrangian section the line segment indicated in red then the period lattice looks like the figure on the right.



The justification for the name *period lattice* comes from the following theorem:

Lemma 2.4.7 (Exercise). *For each $b \in U$, the intersection $\Lambda_b = \Lambda \cap (\{b\} \times \mathbf{R}^n)$ is a lattice in \mathbf{R}^n , that is a discrete subgroup of \mathbf{R}^n . The rank of the lattice is lower semicontinuous as a function of b , that is, b has a neighbourhood V such that $\text{rank}(\Lambda_{b'}) \geq \text{rank}(\Lambda_b)$ for all $b' \in V$.*

Example 2.4.8. In Example 2.4.6, the period lattice for most orbits is isomorphic to \mathbf{Z} , but where U intersects the separatrix orbit the period lattice is the zero lattice.

Recall the following result from differential topology.

Theorem 2.4.9. *If $\Lambda \subset \mathbf{R}^n$ is a lattice then there is a basis e_1, \dots, e_n of \mathbf{R}^n such that Λ is the \mathbf{Z} -linear span of the vectors e_1, \dots, e_k for some $k \leq n$.*

Our next goal is to find a local diffeomorphism $G: U \rightarrow \mathbf{R}^n$ such that $G \circ H$ has standard period lattice.

2.5 The Arnol'd-Liouville theorem

Theorem 2.5.1 (Little Arnol'd-Liouville theorem). *Let $H: X \rightarrow \mathbf{R}^n$ be an integrable Hamiltonian system and $\sigma: U \rightarrow X$ be a local Lagrangian section. Each orbit $\text{Orb}(\sigma)$ is diffeomorphic to $(\mathbf{R}^k/\mathbf{Z}^k) \times \mathbf{R}^{n-k}$ for some k . In particular, if $\text{Orb}(\sigma)$ is compact then it is a torus.*

Proof. The action of \mathbf{R}^n defines a diffeomorphism $\mathbf{R}^n/\Lambda_\sigma \rightarrow \text{Orb}(\sigma)$. Since Λ_σ is a lattice, the result follows from the classification of lattices in Theorem 2.4.9. \square

We now focus attention on a neighbourhood of a compact (torus) orbit. By Lemma 2.4.7, all nearby orbits are also tori. We will

shrink the domain U of our local Lagrangian section so that all orbits through $\sigma(U)$ are compact and, moreover, so that U is a disc.

Theorem 2.5.2 (Action-angle coordinates). *There is a local change of coordinates $G: U \rightarrow \mathbf{R}^n$ such that $G \circ H: H^{-1}(U) \rightarrow \mathbf{R}^n$ generates a Hamiltonian torus action on $H^{-1}(U)$. In other words, the period lattice Λ is standard, equal to $U \times (2\pi\mathbf{Z})^n$ and the map $\Psi: U \times \mathbf{R}^n \rightarrow X$ defined in Theorem 2.4.3 descends to give a symplectomorphism $U \times (\mathbf{R}/2\pi\mathbf{Z})^n \rightarrow H^{-1}(U)$.*

Proof. The following proof is due to Duistermaat [5].

For each $b \in U$, let $2\pi W_1(b), \dots, 2\pi W_n(b) \in \mathbf{R}^n$ be a collection of vectors (smoothly varying in b) which span the lattice of periods Λ_b . We wish to find functions $G_1(b_1, \dots, b_n), \dots, G_n(b_1, \dots, b_n)$ such that $\iota_{W_i}\omega = -d(G_i \circ H)$. If $W_i = \sum \alpha_{ij} V_{H_j}$ then this is equivalent to requiring $\frac{\partial G_i}{\partial b_j} = \alpha_{ij}$. By the Poincaré lemma, we can find such functions G_i provided

$$\frac{\partial \alpha_{ij}}{\partial b_k} = \frac{\partial \alpha_{ik}}{\partial b_j}, \quad (2.2)$$

so it remains to check this identity.

Let $\Psi: U \times \mathbf{R}^n \rightarrow X$ be the Liouville coordinates and $\Lambda = \Psi^{-1}(\sigma(U))$ be the period lattice. Since Ψ is symplectic and $\sigma(U)$ is Lagrangian, Λ is Lagrangian. Moreover, Λ is a union of sheets, each traced out by a single lattice point. For example, $\{(b, W_i(b)) : b \in U\}$ traces out a Lagrangian sheet for each i . In coordinates, this is $\{(b_1, \dots, b_n, \alpha_{i1}(b), \dots, \alpha_{in}(b)) : b \in U\}$, which is Lagrangian if and only if Equation (2.2) holds. \square

Definition 2.5.3. The Liouville coordinates associated to the new, periodic Hamiltonian system are called *action-angle coordinates*. More precisely, the new Hamiltonians $G_1 \circ H, \dots, G_n \circ H$ are called *action coordinates* and the new 2π -periodic conjugate coordinates t_1, \dots, t_n are called *angle coordinates*.

Corollary 2.5.4 (Big Arnol'd-Liouville theorem). *If $H: M \rightarrow \mathbf{R}^n$ is an integrable Hamiltonian system and $\text{Orb}(p)$ is a compact orbit then $\text{Orb}(p)$ is a torus and there is a neighbourhood of $\text{Orb}(p)$ symplectomorphic to $U \times T^n$, where $U \subset \mathbf{R}^n$ is an open ball and the symplectic form is given by $\sum_{i=1}^n db_i \wedge dt_i$. Under this symplectomorphism, the orbits of the original system are sent to the tori $\{b\} \times T^n$.*

2.6 Exercises

Exercise 2.6.1. Let (p, q) be coordinates on $\mathbf{R} \times S^1$ (with $q \in \mathbf{R}/2\pi\mathbf{Z}$) and let $\omega = dp \wedge dq$. Consider the Hamiltonian $H = \frac{1}{2}p^2 + \cos q$. Find its critical points and the Hessian of H at the critical points. Sketch the level sets of H and identify the orbits of ϕ_t^H . Physically, this Hamiltonian system corresponds to a pendulum swinging in a uniform gravitational field; q is the angular displacement from the downward vertical. What is the physical interpretation of the orbits you identified? Around the critical point $(0, 0)$, make the *small angle approximation* $\cos q \approx 1 - \frac{q^2}{2}$ and solve the resulting Hamiltonian system. Verify Galileo's observation that the period of a pendulum with small oscillation is independent of its initial angular displacement. ** Find the period precisely in terms of elliptic integrals.

Exercise 2.6.2. Show that in the local model $H: \mathbf{R}^n \times (\mathbf{R}/2\pi\mathbf{Z})^n \rightarrow \mathbf{R}^n$, $H(p, q) = p$, the action coordinates of the orbit $O_b := H^{-1}(b)$ are $\left(\frac{1}{2\pi} \int_{c_1} \lambda_0, \dots, \frac{1}{2\pi} \int_{c_n} \lambda_0\right)$ where $\lambda_0 = \sum_{k=1}^n p_k dq_k$ and c_k is the loop $\{p = 0, q_i = 0 \text{ for } i \neq k\}$. Verify that the same is true for any λ satisfying $d\lambda = \omega$.

Exercise 2.6.3. Consider the unit 2-sphere (S^2, ω) where ω is the area form. By comparing infinitesimal area elements, show that the projection map from S^2 to a circumscribed cylinder is area-preserving⁵. Let $H: S^2 \rightarrow \mathbf{R}$ be the height function $H(x, y, z) = z$ (thinking of S^2 embedded in the standard way in \mathbf{R}^3). Show that H is an action coordinate.

Exercise 2.6.4. A *symplectic vector space* is a vector space X together with a nondegenerate alternating bilinear form ω (like the tangent space of a symplectic manifold). A subspace $Y \subset X$ is called:

⁵If Cicero is to be believed, a diagram representing this theorem was engraved on the tomb of Archimedes (who proved it).

- *symplectic* if $\omega|_Y$ is symplectic;
- *isotropic* if $\omega|_Y = 0$.

Given a subspace Y , define the symplectic orthogonal complement

$$Y^\omega := \{v \in X : \omega(v, w) = 0 \text{ for all } w \in Y\}.$$

A basis $p_1, q_1, \dots, p_n, q_n$ for X is called *symplectic* if $\omega(p_j, q_k) = \delta_{jk}$ and $\omega(p_j, p_k) = \omega(q_j, q_k) = 0$ for all j, k . Show that: a) any symplectic vector space admits a symplectic basis and hence has even dimension. (Hint: Work inductively using symplectic orthogonal complement.) b) if Y is isotropic then $Y \subset Y^\omega$. Deduce that $\dim Y \leq n$.

Exercise 2.6.5. If F and G are two functions on a symplectic manifold, define $F_t(x) = F(\phi_t^G(x))$ and show that $\dot{F}_t = \{G, F_t\}$.

Exercise 2.6.6. Recall that the flows along two vector fields commute if and only if the Lie bracket of the vector fields vanishes. Deduce that two Hamiltonian flows ϕ_t^F and ϕ_t^G commute if and only if the Poisson bracket $\{F, G\}$ is locally constant.

Exercise 2.6.7. Darboux's theorem states that for any symplectic $2n$ -manifold (X, ω) and any point $x \in X$, there are coordinates $(p_1, q_1, \dots, p_n, q_n)$ centred on x such that $\omega = \sum dp_i \wedge dq_i$ in these coordinates. We will prove this by induction. This proof is from Arnol'd's book [1, Section 43.B] (look there if you get stuck). As so often in geometry proofs, we will tacitly pass to a smaller neighbourhood at various points in the proof. a) Pick a function p_1 and let N be a submanifold passing through x , transverse to the vector field V_{p_1} in a neighbourhood of x . For points in a neighbourhood of x , define q_1 to be the unique number such that $\phi_{-q_1}^{p_1}(x) \in N$. Compute the Lie derivative $L_{V_{p_1}} q_1$ and show that $\{p_1, q_1\} = 1$. Deduce that the flows $\phi_t^{p_1}$ and $\phi_t^{q_1}$ commute. Deduce Darboux's theorem in the case $n = 1$. b) Let $M = \{p_1 = q_1 = 0\}$. Why is $T_x M$ a symplectic subspace of $T_x X$? Why does this mean that M is a symplectic submanifold in a neighbourhood of x ? c) By induction, M admits

Darboux coordinates $(a_2, b_2, \dots, a_n, b_n)$ in a neighbourhood of x . Any point x' in a neighbourhood of x can be written uniquely as $x' = \phi_s^{p_1} \phi_t^{q_1}(m(x'))$ with $m(x') \in M$, so defining $p_k(x') = a_k(m(x'))$ and $q_k(x') = b_k(m(x'))$ we get coordinates $(p_1, q_1, \dots, p_n, q_n)$ on a neighbourhood of x . Check that these are Darboux coordinates, in other words: $\{p_j, q_k\} = \delta_{jk}$, $\{p_j, p_k\} = \{q_j, q_k\} = 0$ for all j, k .

Exercise 2.6.8. There always exists a local Lagrangian section through any regular point x of an integrable Hamiltonian system.

Exercise 2.6.9. Suppose that $H: X \rightarrow \mathbf{R}$ is a Hamiltonian function and $L \subset X$ is a Lagrangian submanifold such that $L \subset H^{-1}(c)$ for some $c \in \mathbf{R}$. Prove that $\phi_t^H(x) \in L$ for all $x \in L$, $t \in \mathbf{R}$, i.e. that L is invariant under the Hamiltonian flow of H .

Exercise 2.6.10. Let (X, ω) be a symplectic $2n$ -manifold, B be an n -manifold and let $\pi: X \rightarrow B$ be a proper submersion with connected Lagrangian fibres. Let (b_1, \dots, b_n) be local coordinates on B . Prove that $b_1 \circ \pi, \dots, b_n \circ \pi$ Poisson commute, and deduce that the fibres of π are Lagrangian tori. This is the reason the words *Lagrangian torus fibration* and *integrable Hamiltonian system* are often conflated (Hint: Use Exercise 2.6.9.)

The final two questions use the fact that the Liouville map Ψ is a local diffeomorphism.

Exercise 2.6.11. Let $H: X \rightarrow \mathbf{R}^n$ be an integrable Hamiltonian system and $\sigma: U \rightarrow X$ be a local Lagrangian section. Let Λ be the associated period lattice. Prove that, for each point $b \in U$, the intersection $\Lambda_b := \Lambda \cap (\{b\} \times \mathbf{R}^n)$ is a sublattice of \mathbf{R}^n (that is, a discrete subgroup of \mathbf{R}^n).

Exercise 2.6.12. Let $H: X \rightarrow \mathbf{R}^n$ be an integrable Hamiltonian system and $\sigma: U \rightarrow X$ be a local Lagrangian section. Show that the function $U \rightarrow \mathbf{Z}$, $b \mapsto \text{rank}(\Lambda_b)$, is lower semi-continuous (in other words, there is an open neighbourhood V of b such that, for $b' \in V$, $\text{rank}(\Lambda_{b'}) \geq \text{rank}(\Lambda_b)$).

Chapter 3

Hamiltonian torus actions

3.1 Global action-angle coordinates

We saw in the last chapter that if $H: X \rightarrow \mathbf{R}^n$ is an integrable Hamiltonian system and b is a regular value then we can postcompose with a local change of coordinates G on a neighbourhood U of b to get a new system $G \circ H$ such that $G \circ H$ generates a torus action on $H^{-1}(U)$. The components $G_1 \circ H, \dots, G_n \circ H$ are called *action coordinates* and the angular coordinates on the torus fibres are called *angle coordinates*. The following lemma tells us that when we have globally defined action-angle coordinates on X , the whole Hamiltonian system can be recovered just from the image of X under the action coordinates.

Lemma 3.1.1. *Assume that $F: X \rightarrow \mathbf{R}^n$ and $G: Y \rightarrow \mathbf{R}^n$ are integrable Hamiltonian systems such that $U := F(X)$ and $V :=$*

$G(Y)$ consist only of regular values. Assume that F and G are action coordinates in each case and that we are given global Lagrangian sections $\sigma: U \rightarrow X$ and $\tau: V \rightarrow Y$. Suppose there is an integral affine transformation $A: \mathbf{R}^n \rightarrow \mathbf{R}^n$ such that $A(U) = V$. There is a symplectomorphism $\Phi: X \rightarrow Y$ such that $G \circ \Phi = A \circ F$; we call such a symplectomorphism fibred.

This is a wonderful compression of information: to reconstruct a $2n$ -dimensional space, all we need is a subset of \mathbf{R}^n . For example, if $n = 2, 3$, this brings 4- and 6-dimensional spaces into the range of visualisation. The goal of the rest of this book is to exploit this in increasing levels of generality.

- In this chapter, we will keep the assumption that there are global action-angle coordinates, but allow for critical points. This will lead us to the study of toric manifolds.
- In Chapter 4, we will drop the assumption that there are global action-angle coordinates and see what remains. We will introduce more general singularities (focus-focus singularities) and study the asymptotics of action-angle coordinates in the neighbourhood of a singular fibre.
- In Chapter 5, we will combine what we have done so far to visualise a range of interesting 4- and 6-dimensional manifolds.
- In Chapter 6, we will explain a construction due to Ruan of integrable Hamiltonian systems on projective varieties admitting toric degenerations. The singularities of these examples are still poorly-understood.

3.2 Hamiltonian group actions

One way of stating the Arnol'd-Liouville theorem is that, after a suitable change of coordinates in the target, the \mathbf{R}^n -action generated by the Hamiltonian vector fields V_{H_1}, \dots, V_{H_n} actually factors

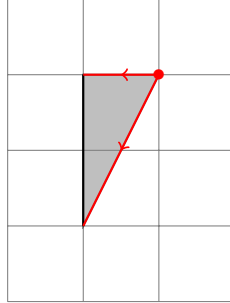
through a T^n -action. We now work backwards, assuming that we have a globally-defined torus action, even on the non-regular fibres, and see what kinds of singularities can occur.

Definition 3.2.1. Let $H: X \rightarrow \mathbf{R}^n$ be an integrable Hamiltonian system such that the Hamiltonian \mathbf{R}^n -action Φ_t^H factors through a Hamiltonian T^n -action, that is $\Phi_t^H = id$ for any $t \in (2\pi\mathbf{Z})^n$. Then we call H the *moment map* for the torus action; this is a synonym for having globally defined action coordinates. We often write μ for a moment map, to distinguish it from a system where the period lattice is not standard.

We saw in Lemma 3.1.1 that the image of a moment map determines the Hamiltonian system completely up to fibred symplectomorphism, at least if there are no critical points and there is a global Lagrangian section. We therefore concentrate on the image $\mu(X)$ of the moment map, which we will call the *moment image* or *moment polytope*. The Atiyah-Guillemin-Sternberg convexity theorem tells us that $\mu(X)$ indeed a polytope. Before stating this theorem, we recall some basic definitions.

Definition 3.2.2. A *rational convex polytope* P is a subset of \mathbf{R}^n defined as the intersection of a finite collection of half-spaces $S_{\alpha,b} = \{x \in \mathbf{R}^n : \alpha_1 x_1 + \cdots + \alpha_n x_n \leq b\}$ with $\alpha_1, \dots, \alpha_n \in \mathbf{Q}$ and $b \in \mathbf{R}$. We say that P is a *Delzant polytope* if it is a convex rational polytope such that every point on a k -dimensional facet has a neighbourhood isomorphic (via an integral affine transformation) to a neighbourhood of the origin in the polytope $[0, \infty)^{n-k} \times \mathbf{R}^k$.

Example 3.2.3. The polygon below fails to be Delzant: there is no integral affine transformation sending the marked vertex to the origin and sending the two marked edges to the x - and y -axes, which would be the Delzant condition for this vertex. Indeed, the primitive integer vectors $\begin{pmatrix} -1 \\ 0 \end{pmatrix}$ and $\begin{pmatrix} -1 \\ -2 \end{pmatrix}$ pointing along these edges span a strict sublattice of the integer lattice \mathbf{Z}^2 .



Theorem 3.2.4 (Atiyah, Guillemin-Sternberg, Delzant). *Let (X, ω) be a symplectic $2n$ -manifold and $\mu: X \rightarrow \mathbf{R}^n$ a moment map for a Hamiltonian T^n -action.*

1. *The image $\Delta := \mu(X)$ is a Delzant polytope.*
2. *If X is compact, then Δ is the convex hull of $\{\mu(x) : x \in \text{Fix}(X)\}$, where $\text{Fix}(X)$ is the set of fixed points of the torus action.*
3. *For any Delzant polytope $\Delta \subset \mathbf{R}^n$ there exists a symplectic $2n$ -manifold X_Δ and a map $\mu: X_\Delta \rightarrow \mathbf{R}^n$ with $\mu(X_\Delta) = \Delta$ such that μ generates a Hamiltonian T^n -action. Moreover, X_Δ is a projective variety. Such varieties are often called projective toric varieties.*
4. *The moment polytope determines X, μ up to fibred symplectomorphism.*

We will not prove this theorem, and will focus instead on extracting geometric information about X from the moment polytope.

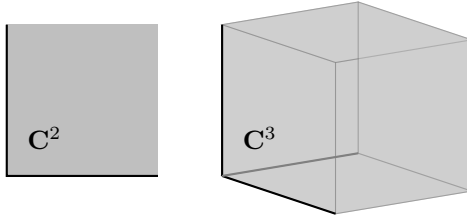
Example 3.2.5. Consider the n -torus action on \mathbf{C}^n given by

$$(z_1, \dots, z_n) \mapsto (e^{it_1} z_1, \dots, e^{it_n} z_n).$$

This is Hamiltonian, with moment map

$$\mu(z_1, \dots, z_n) = \left(\frac{1}{2}|z_1|^2, \dots, \frac{1}{2}|z_n|^2 \right).$$

The image of the moment map is the nonnegative orthant. This is a manifold with boundary and corners: the μ -preimage of a boundary stratum of codimension k is an $(n - k)$ -dimensional torus. For example, the preimage of the vertex is a single fixed point (the origin), the preimage of a point on the positive x_1 -axis is a circle with fixed radius in the z_1 -plane, the preimage of a point on the interior of the x_1x_2 -plane is a 2-torus, and so forth.



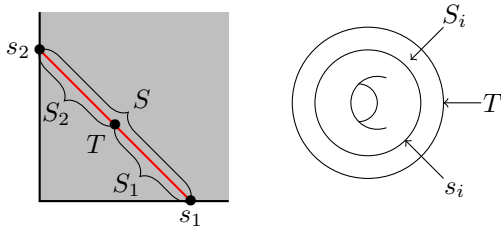
Remark 3.2.6. The critical values of μ are precisely the boundary points of the moment polytope. The boundary is stratified into facets of dimension 0 (vertices), 1 (edges), 2 (faces), etc, so we can classify the critical values according to the dimension of the stratum to which they belong. By definition, any Delzant polytope is locally isomorphic to $\mathbf{R}^k \times [0, \infty)^{n-k}$ in a neighbourhood of a point in a k -dimensional facet. In Example 3.2.5, we have found a system whose moment image is $[0, \infty)^{n-k}$, so by Theorem 3.2.4(4), this means that the integrable Hamiltonian system in a neighbourhood of a critical point living over a k -dimensional facet is fibred-symplectomorphic to the system

$$\begin{aligned} \mu: \mathbf{R}^k \times (S^1)^k \times \mathbf{C}^{n-k} &\rightarrow \mathbf{R}^n, \\ \mu(p, q, z_{k+1}, \dots, z_n) &= \left(p, \frac{1}{2}|z_{k+1}|^2, \dots, \frac{1}{2}|z_n|^2 \right). \end{aligned}$$

Such singularities are called *toric*¹ and the set of all toric singularities is often called the *toric boundary* of X . It is not a boundary in the usual sense: it is a union of submanifolds of codimension 2. Instead, considering X as a projective variety, it is the boundary in the sense of algebraic geometry: it is a divisor, and is often called the *toric divisor*.

Our ultimate goal is to see features of the geometry laid bare via the moment map. As an example of what we have in mind, here is a nice way to understand the genus 1 Heegaard decomposition of the 3-sphere using the moment map for \mathbf{C}^2 .

Example 3.2.7. Let $\mu: \mathbf{C}^2 \rightarrow \mathbf{R}^2$ be the moment map from Example 3.2.5. The preimage of the (red) line segment $x_1 + x_2 = \frac{1}{2}$, $x_1, x_2 \geq 0$, is the subset $S := \{(z_1, z_2) \in \mathbf{C}^2 : |z_1|^2 + |z_2|^2 = 1\}$, that is the unit 3-sphere. The fibre $T := \mu^{-1}(\frac{1}{4}, \frac{1}{4})$ is a torus with $T \subset S$. We can see that T separates S into two pieces S_1, S_2 , and it is also easy to see that each piece is homeomorphic to a *solid torus* $S^1 \times D^2$: the “core circles” of these solid tori are the fibres $s_1 = \mu^{-1}(\frac{1}{2}, 0)$, $s_2 = \mu^{-1}(0, \frac{1}{2})$ where the line segment intersects the x_1 - and x_2 -axes.



¹In fact, it is a theorem of Eliasson [6] and Dufour–Molino [4] that toric singularities can be characterised purely in terms of the Hessian of the Hamiltonian system at the singular point. They call such critical points *elliptic*.

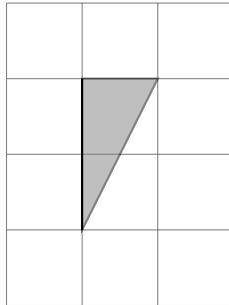
3.3 Examples

Example 3.3.1. We saw in Exercise 2.6.3 that the height function on the unit 2-sphere in \mathbf{R}^3 generates a Hamiltonian circle action (i.e. T^1 -action). The image of the moment map is the interval $[-1, 1]$. One can form more examples by taking products: we get a T^n -action on $(S^2)^n$, whose moment map is $\mu((x_1, y_1, z_1), \dots, (x_n, y_n, z_n)) = (z_1, \dots, z_n)$, with image $[-1, 1]^n$. For example, the moment image for $S^2 \times S^2$ is a square, for $S^2 \times S^2 \times S^2$ it is a cube.

Example 3.3.2. If we take S^2 with the area form $\lambda\omega$ (where ω is the form giving area 4π) then the rescaled height function λz is a moment map for the circle action which rotates around the z -axis with period 2π . The moment image is $[-\lambda, \lambda]$.

Definition 3.3.3 (Affine length). If $\ell: [0, L] \rightarrow \mathbf{R}^n$ is a line segment of the form $\ell(t) = at + b$ with $a = \begin{pmatrix} a_1 \\ a_2 \end{pmatrix} \in \mathbf{Z}^2$, $\gcd(a_1, a_2) = 1$ and $b \in \mathbf{R}^n$ then we say ℓ is a *rational* line segment and the *affine length* of ℓ is defined to be L .

Example 3.3.4. In the polygon below, the vertical edge has affine length 2 and the other two edges both have affine length 1.



Lemma 3.3.5. If $\ell: [0, L] \rightarrow \mathbf{R}^n$ is a rational line segment whose image is an edge of the moment polytope then $\mu^{-1}(\ell([0, L]))$ is a

symplectic sphere of symplectic area $2\pi L$.

Proof. By Theorem 3.2.4(4), the preimage of such an edge is precisely symplectomorphic to $(S^2, \frac{L\omega}{2})$ with a rescaling of its height function by $L/2$, by comparing with Example 3.3.2. □

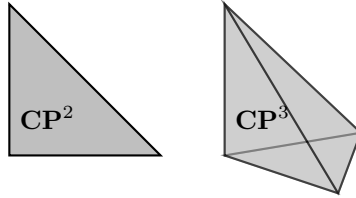
Example 3.3.6. Consider the complex projective n -space \mathbf{CP}^n , with homogeneous coordinates $[z_1 : \cdots : z_{n+1}]$. This has a torus action $[z_1 : \cdots : z_{n+1}] \mapsto [e^{it_1} z_1 : \cdots : e^{it_n} z_n : z_{n+1}]$ which is Hamiltonian, for the Fubini-Study form ω , with moment map

$$\mu([z_1 : \cdots : z_{n+1}]) = \left(\frac{1}{2} \frac{|z_1|^2}{|z|^2}, \dots, \frac{1}{2} \frac{|z_n|^2}{|z|^2} \right),$$

where $|z|^2 = \sum_{i=1}^{n+1} |z_i|^2$. The moment image is the simplex

$$\{(x_1, \dots, x_n) \in \mathbf{R}^n : x_1, \dots, x_n \geq 0, x_1 + \cdots + x_n \leq 1\}.$$

For example, $\mu(\mathbf{CP}^2)$ and $\mu(\mathbf{CP}^3)$ are drawn below. In each case, the *hyperplane at infinity* $\{[z_1 : \cdots : z_n : 0]\}$ projects via μ to the facet $x_1 + \cdots + x_n = 1$ of the simplex.



Example 3.3.7. The *tautological bundle* over \mathbf{CP}^1 is the variety

$$\mathcal{O}(-1) := \{(x, y, [a : b]) \in \mathbf{C}^2 \times \mathbf{CP}^1 : ay = bx\}.$$

This has a holomorphic projection $\pi: \mathcal{O}(-1) \rightarrow \mathbf{CP}^1$, $\pi(x, y, [a : b]) = [a : b]$, which exhibits it as the total space of a holomorphic line bundle over \mathbf{CP}^1 . This is a fancy way of saying that $\pi^{-1}([a : b])$

is a complex line (specifically $\{(x, y) \in \mathbf{C}^2 : ay = bx\} \subset \mathbf{C}^2$) for all $[a : b] \in \mathbf{CP}^1$. The symplectic form $\omega_{\mathbf{C}^2} \oplus \omega_{\mathbf{CP}^1}$ on $\mathbf{C}^2 \times \mathbf{CP}^1$ pulls back to a symplectic form on $\mathcal{O}(-1)$, with respect to which the following T^2 -action is Hamiltonian:

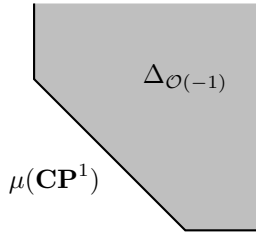
$$(x, y, [a : b]) \mapsto (e^{it_1}x, e^{it_2}y, [e^{it_1}a : e^{it_2}b]).$$

The moment map is

$$\mu(x, y, [a : b]) = \left(\frac{1}{2} \left(|x|^2 + \frac{|a|^2}{|a|^2 + |b|^2} \right), \frac{1}{2} \left(|y|^2 + \frac{|b|^2}{|a|^2 + |b|^2} \right) \right).$$

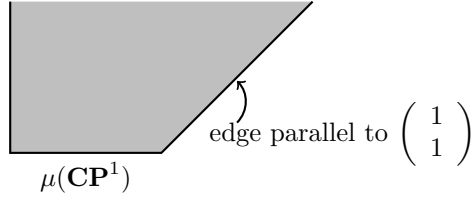
The image of the moment map is the subset

$$\Delta_{\mathcal{O}(-1)} := \left\{ (x_1, x_2) \in \mathbf{R}^2 : x_1, x_2 \geq 0, x_1 + x_2 \geq \frac{1}{2} \right\}.$$



The zero-section $\mathbf{CP}^1 = \{x = y = 0\} \subset \mathcal{O}(-1)$ projects down to the edge $x_1 + x_2 = \frac{1}{2}$. An alternative moment map can be obtained by postcomposing with the integral affine transformation $\begin{pmatrix} x_1 \\ x_2 \end{pmatrix} \mapsto \begin{pmatrix} 1 & 0 \\ 1 & 1 \end{pmatrix} \begin{pmatrix} x_1 \\ x_2 \end{pmatrix} + \begin{pmatrix} 0 \\ -1 \end{pmatrix}$, which sends the moment polytope to

$$\{(x_1, x_2) \in \mathbf{R}^2 : x_1, x_2 \geq 0, x_1 - x_2 \geq -1\}.$$



This is an important example because of the role played by $\mathcal{O}(-1)$ in birational geometry. The projection $\varpi: \mathcal{O}(-1) \rightarrow \mathbf{C}^2$ given by $\varpi(x, y, [a : b]) = (x, y)$ is the *blow-down* map: it is an isomorphism away from $(0, 0) \in \mathbf{C}^2$, but it contracts the sphere $\{(0, 0, [a : b]) : [a : b] \in \mathbf{CP}^1\}$ (known as the *exceptional sphere*) to the origin. In fact, if we take a toric variety X_Δ and blow-up a fixed point of the torus action (living over a vertex $v \in \Delta$), we get a new toric variety $X_{\Delta'}$ whose moment polytope Δ' differs from the previous one by truncating at the vertex v . More precisely, we use an integral affine transformation to put Δ in such a position that v sits at the origin and Δ is locally isomorphic to $[0, \infty)^n$ near v , then we truncate Δ using the hyperplane $x_1 + \cdots + x_n = c$ for some positive c . Varying the constant c will give different symplectic structures (in particular, for $n = 2$, the symplectic area of the exceptional sphere will vary).

Example 3.3.8. The bundle $\mathcal{O}(-n)$ over \mathbf{CP}^1 is the variety²

$$\mathcal{O}(-n) := \{(x, y, [a : b]) \in \mathbf{C}^2 \times \mathbf{CP}^1 : a^n y = b^n x\}$$

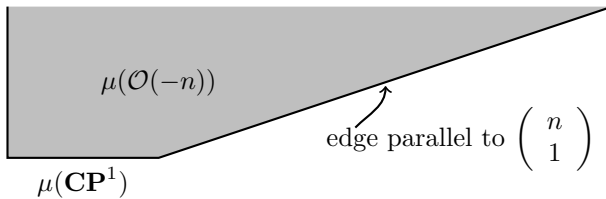
The Hamiltonians

$$H_1 = \frac{1}{2} \left(|x|^2 + \frac{|a|^2}{|a|^2 + |b|^2} \right), \quad H_2 = \frac{1}{2} \left(|y|^2 + \frac{|b|^2}{|a|^2 + |b|^2} \right)$$

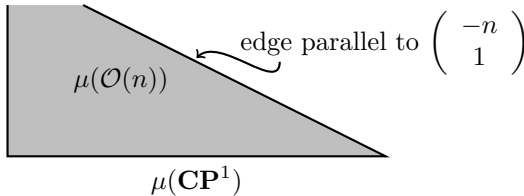
still generate circle actions, but the period lattice for the \mathbf{R}^2 -action generated by (H_1, H_2) , while constant, is no longer standard: the element $\phi_{2\pi/n}^{H_1} \phi_{2\pi/n}^{H_2}$ now acts as the identity. This means that the

²The discerning reader will spot that this is the pullback of $\mathcal{O}(-1)$ along the degree n holomorphic map $\mathbf{CP}^1 \rightarrow \mathbf{CP}^1$, $[a : b] \mapsto [a^n : b^n]$.

period lattice is spanned by $\mathbf{Z} \begin{pmatrix} 2\pi/n \\ 2\pi/n \end{pmatrix} \oplus \mathbf{Z} \begin{pmatrix} 2\pi \\ 0 \end{pmatrix}$. If we use the combination $\mu = (H_1, \frac{H_1+H_2}{n})$ then we get a standard period lattice, so this is the correct moment map. To find the moment image, we simply apply the affine transformation $\begin{pmatrix} 1 & 0 \\ 1/n & 1/n \end{pmatrix}$ to $\Delta_{\mathcal{O}(-1)}$ (we also translate it by $\begin{pmatrix} 0 \\ -1/n \end{pmatrix}$ so that the horizontal edge $\mu(\mathbf{CP}^1)$ sits on the x_1 -axis).



Similarly, one can define the bundles $\mathcal{O}(n) \rightarrow \mathbf{CP}^1$, $n \geq 0$, and these admit torus actions; the moment map now sends a neighbourhood of the zero-section in $\mathcal{O}(n)$ to a region as shown below. For example, a complex line in \mathbf{CP}^2 has normal bundle $\mathcal{O}(1)$, and in the moment image of \mathbf{CP}^2 we see precisely the $n = 1$ neighbourhood surrounding the x_1 -axis.



The following lemma now follows immediately from these examples and Theorem 3.2.4(4).

Lemma 3.3.9. *Let $\Delta \subset \mathbf{R}^2$ be a moment polygon and $e \subset \Delta$ an edge connecting two vertices P, Q . Assume that this edge is tra-*

versed from P to Q as you move anticlockwise around the boundary of Δ . Let v, w be primitive integer vectors pointing along the other edges emerging from P and Q respectively. Then a neighbourhood of $\mu^{-1}(e)$ in X_Δ is symplectomorphic to a neighbourhood of the zero-section in $\mathcal{O}(n)$ where $n = \det M$ where M is the matrix with columns v, w .

Proof. This is true for the local model discussed above, and any edge is integral affine equivalent to one of these local models. Moreover, the determinant is preserved by integral affine transformations which preserve the orientation of the plane (and hence the anticlockwise sense of traversing the boundary). An orientation-reversing transformation will switch the sign of the determinant and also switch the order of the columns because it switches anticlockwise to clockwise, so these sign effects will cancel.

□

3.4 Visible Lagrangian submanifolds

The action-angle coordinates are usually difficult to find explicitly as they involve performing integrals. Even some of the simplest Hamiltonian systems (like the pendulum) have action-angle coordinates which involve elliptic functions. For that reason, we would like a way to see some of the affine geometry of the action coordinates without having to find them explicitly. We will see now that Lagrangian submanifolds which fibre in a nice way via the Hamiltonians of the system always project to an affine linear subspace in an action coordinate patch.

Theorem 3.4.1 (Symington [10, Theorem ?]). *Consider the integrable Hamiltonian system $H: (\mathbf{R}^n \times T^n, \sum dp_i \wedge dq_i) \rightarrow \mathbf{R}^n$, $H(p, q) = p$ where q_1, \dots, q_n are taken modulo 2π . Let $L \subset \mathbf{R}^n \times T^n$ be a Lagrangian submanifold. Suppose that $H|_L: L \rightarrow \mathbf{R}^n$ factors*

as $H|_L = f \circ g$, where $g: L \rightarrow K$ is a bundle over a k -dimensional manifold K , $k < n$, and $f \circ K \rightarrow \mathbf{R}^n$ is an embedding. Then K is an affine linear subspace of \mathbf{R}^n which is rational with respect to the lattice $(2\pi\mathbf{Z})^n$.

Definition 3.4.2. We call such Lagrangian submanifolds *visible*.

Proof. Let $s = (s_1, \dots, s_k)$ be local coordinates on K and (t_{k+1}, \dots, t_n) be local coordinates on the fibre of g . By assumption, the inclusion of L into \mathbf{R}^n has the form $(s, t) \mapsto (p(s), q(s, t))$ for some functions. The vectors ∂_{s_i} and ∂_{t_j} pushforward to $(\partial_{s_i}p, \partial_{s_i}q)$ and $(0, \partial_{t_j}q)$. The Lagrangian condition on L is equivalent to $\partial_{s_i}p \cdot \partial_{t_j}q = 0$ for all i, j and $\partial_{s_i}p \cdot \partial_{s_j}q = \partial_{s_j}p \cdot \partial_{s_i}q$. The first of these conditions implies that the tangent space of the fibre of g is orthogonal to the k -dimensional subspace $f_*(TK)$ spanned by $\partial_{s_1}p, \dots, \partial_{s_k}p$. Since the tangent space of the fibre of g is $(n - k)$ -dimensional, it must be precisely $f_*(TK)^\perp$; in other words, for each $s \in K$, the fibre of g over s is an integral submanifold of the distribution on T^n given by $f_*(TK)^\perp$. This distribution has an integral submanifold if and only if $f_*(TK)$ is a rational subspace with respect to the lattice $(2\pi\mathbf{Z})^n$. Since $f_*(TK)$ varies smoothly in s , and must always be rational, it is necessarily constant. Therefore $f(K)$ is a rational affine subspace. \square

Remark 3.4.3. Note that the dependence of q_i on the coordinates s_j can be nontrivial.

Example 3.4.4. Let (p_1, p_2, q_1, q_2) be coordinates on $X = \mathbf{R}^2 \times (S^1)^2$ with symplectic form $\sum dp_i \wedge dq_i$. The Lagrangian embedding $i: \mathbf{R} \times S^1 \rightarrow X$, $i(s, t) = (s, 0, 0, t)$ is visible for the projection $(p, q \mapsto p)$. The Lagrangian torus $j: S^1 \times S^1 \rightarrow X$, $j(s, t) = (\sin s, 0, s, t)$ is also visible³, and projects to the line segment $[-1, 1] \times \{0\}$ (the preimage of each point in $(-1, 1) \times \{0\}$ is a pair of circles).

³Technically, it is not visible itself because the projection map is not a bundle, rather it is a union of two visible cylinders. We will tolerate this and related abuses of terminology.

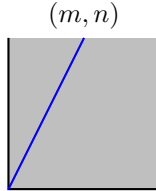
3.4.1 Hitting a vertex

We now suppose that we have a Hamiltonian torus action (and toric singularities) with moment map $\mu: X \rightarrow \mathbf{R}^n$ and address the question of what visible Lagrangian surfaces look like when the linear subspace $\mu(L)$ intersects the boundary strata of the moment polytope. For simplicity, we will focus on the case $\dim X = 4$, $\dim \mu(L) = 1$.

Example 3.4.5 (Exercise). Consider the Lagrangian plane $L := \{(z, \bar{z}) : z \in \mathbf{C}\} \subset \mathbf{C}^2$. The projection $\mu(L)$ is the diagonal ray $\{(t, t) : t \in [0, \infty)\} \subset \mathbf{R}^2$, so L is a visible Lagrangian surface. If we look more generally over the ray $\{(mt, nt) : t \in [0, \infty)\}$ (blue in the figure below), with $m, n \in \mathbf{Z}$, $\gcd(m, n) = 1$, we find the *Schoen-Wolfson cone*⁴

$$(r, \theta) \mapsto \frac{1}{\sqrt{m+n}} \left(r\sqrt{n}e^{i\theta\sqrt{m/n}}, ir\sqrt{m}e^{-i\theta\sqrt{n/m}} \right),$$

which is singular at the origin unless $m = n = 1$.



Modulo the freedom discussed in Remark 3.4.3 and Example 3.4.4, this exhausts all possible local models for visible Lagrangians living over a line which hits the corner of a Delzant moment polygon.

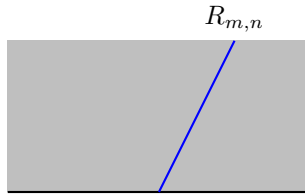
⁴Schoen and Wolfson [8, Theorem 7.1] showed that these are the only Lagrangian cones in \mathbf{C}^2 which are Hamiltonian stationary (i.e. critical points of the volume functional restricted to Hamiltonian deformations).

3.4.2 Hitting an edge

Example 3.4.6. We now consider visible Lagrangians whose projection hits an edge. For a local model, we take $X = \mathbf{R} \times S^1 \times \mathbf{C}$, with coordinates $(p, q, z = x + iy)$ ($q \in \mathbf{R}/2\pi\mathbf{Z}$) and symplectic form $dp \wedge dq + dx \wedge dy$. The moment map $\mu: X \rightarrow \mathbf{R}^2$, $\mu(p, q, z) = (p, \frac{1}{2}|z|^2)$, has image the closed upper half-plane $\{(x_1, x_2) \in \mathbf{R}^2 : x_2 \geq 0\}$. Consider the ray $R_{m,n} = \{(ms, ns) : s \geq 0\}$. The following map is a Lagrangian immersion of the cylinder

$$i(s, t) = \left(ms, -nt, \sqrt{2nse^{imt}} \right), \quad (s, t) \in [0, \infty) \times S^1$$

whose projection along μ is the ray $R_{m,n}$. This immersion is an embedding away from $s = 0$, but it is n -to-1 along the circle $s = 0$ (the points $(0, t + \frac{2\pi k}{n})$, $k = 0, \dots, n-1$, all project to $(0, t \bmod 2\pi, 0)$).

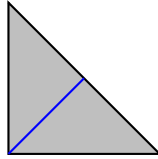


The image of the immersion is a Lagrangian which looks like a collection of n flanges meeting along a circle, twisting as they move around the circle so that the link of the circle is an (m, n) -torus knot. For example, when $m = 1$, $n = 2$, this is a Möbius strip. For $n \geq 3$ it is not a submanifold. We call the image of the immersion a *Lagrangian (n, m) -pinwheel core*.

Any integral affine transformation preserving the upper half-plane and fixing the origin acts on the set of rays $R_{m,n}$. These transformations are precisely the affine shears $\begin{pmatrix} 1 & k \\ 1 & 0 \end{pmatrix}$, which allow us to change m by any multiple of n , so we can always assume $m \in \{0, \dots, n-1\}$.

Again, modulo the freedom discussed in Remark 3.4.3 and Example 3.4.4, these local models exhaust the visible Lagrangians intersecting an edge of a moment polygon.

Example 3.4.7. Consider the Lagrangian \mathbf{RP}^2 which is the closure of the visible disc $\{[z : \bar{z} : 1] : z \in \mathbf{C}\} \subset \mathbf{CP}^2$. This projects to the diagonal bisector in the moment triangle. If we use the integral affine transformation $\begin{pmatrix} -1 & 0 \\ -1 & -1 \end{pmatrix}$ to make the slanted edge of the triangle horizontal then the projection of the visible Lagrangian ends up pointing in the $\begin{pmatrix} 1 \\ 2 \end{pmatrix}$ -direction, which shows that the disc is capped off with a Möbius strip to give an \mathbf{RP}^2 .



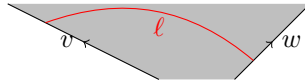
3.5 Exercises

Exercise 3.5.1. Assume that $F: X \rightarrow \mathbf{R}^n$ and $G: Y \rightarrow \mathbf{R}^n$ are integrable Hamiltonian systems such that $U := F(X)$ and $V := G(Y)$ consist only of regular values. Assume that F and G are action coordinates in each case and that we are given global Lagrangian sections $\sigma: U \rightarrow X$ and $\tau: V \rightarrow Y$. Suppose there is an integral affine transformation $A: \mathbf{R}^n \rightarrow \mathbf{R}^n$ such that $A(U) = V$. Show that there is a symplectomorphism $\Phi: X \rightarrow Y$ such that $G \circ \Phi = A \circ F$; we call such a symplectomorphism *fibred*. (Hint: The fibredness condition means that you only need to specify Φ in the angle-directions; it should also be integral affine in these directions.)

Exercise 3.5.2. Consider the group of n th roots of unity μ_n act-

ing on \mathbf{C}^2 via $(z_1, z_2) \mapsto (\mu z_1, \mu^m z_2)$ where $\gcd(m, n) = 1$. Let $X = \mathbf{C}^2/\mu_n$ be the quotient by this group action. This is a symplectic *orbifold*: the origin is a singular point. Nonetheless, provided they fix the origin, Hamiltonian flows still make perfect sense. Find the lattice of periods for the \mathbf{R}^2 -action on X generated by the Hamiltonians $H_1 = \frac{1}{2}|z_1|^2$ and $H_2 = \frac{1}{2}|z_2|^2$ and hence find the moment polygon. Confirm that this fails to be Delzant at its vertex (corresponding to the fact that X is non-smooth). *These singularities are called cyclic quotient singularities.*

Exercise 3.5.3. The cyclic group action from Exercise 3.5.2 preserves the unit sphere in \mathbf{C}^2 , and the quotient S^3/μ_n is the 3-manifold known as the *lens space* $L(n, m)$. Show that lens spaces admit genus 1 Heegaard splittings. If ℓ is a curve segment in a moment polygon which connects two edges such that the edges point in the directions v and w , find an expression in terms of v, w for the numbers m, n such that the preimage $\mu^{-1}(\ell)$ is diffeomorphic to the lens space $L(n, m)$.



Exercise 3.5.4. Verify that the Schoen-Wolfson cone, parametrised by

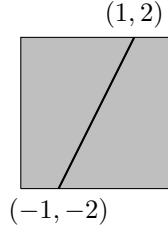
$$(r, \theta) \mapsto \frac{1}{\sqrt{m+n}} \left(r\sqrt{n}e^{i\theta\sqrt{m/n}}, ir\sqrt{m}e^{-i\theta\sqrt{n/m}} \right),$$

is Lagrangian (at least away from its cone point, where the Lagrangian condition makes sense). Check that its projection along the moment map is the ray from the origin pointing in the (m, n) -direction.

Exercise 3.5.5. Consider the Lagrangian *antidiagonal sphere* $\bar{\Delta} := \{((x, y, z), (-x, -y, -z)) \in S^2 \times S^2 : (x, y, z) \in S^2\}$. Find the projection $\mu(\bar{\Delta}) \subset [-1, 1] \times [-1, 1]$.

Exercise 3.5.6. The square below has vertices at $(-2, -2)$, $(-2, 2)$,

$(2, -2)$, $(2, 2)$. There is a smooth, closed visible Lagrangian surface L in the corresponding toric variety, living over the line segment connecting $(-1, -2)$ to $(1, 2)$. To which topological surface is L homeomorphic?



Exercise 3.5.7. Consider the symplectic manifold $\mathbf{CP}^1 \times \mathbf{C}^2$ with the symplectic form $pr_1^* \omega_{\mathbf{CP}^1} + pr_2^* \omega_{\mathbf{C}^2}$ (pr_k denotes the projection to the k th factor, $\omega_{\mathbf{CP}^1}$ is the Fubini-Study form on \mathbf{CP}^1 normalised so that $\frac{1}{2\pi} \int_{\mathbf{CP}^1} \omega_{\mathbf{CP}^1} = 1$ and $\omega_{\mathbf{C}^2}$ is the standard symplectic form). Sketch the moment image for the T^3 -action coming from the standard torus actions on each factor. Check that the 3-sphere $\{([-z_2 : z_1], (z_1, z_2) : |z_1|^2 + |z_2|^2 = 1\} \subset \mathbf{CP}^1 \times \mathbf{C}^2$ is Lagrangian and sketch its projection under the moment map.

Exercise 3.5.8. Consider the map

$$F: (\mathbf{C}^*)^2 \rightarrow \mathbf{CP}^3, \quad F(x, y) = [xy : x : y : 1].$$

Show that the Zariski-closure of the image of F is a quadric surface Q . Let $\mu: \mathbf{CP}^3 \rightarrow \mathbf{R}^3$ be the moment map for the standard T^3 -action. Find a subtorus $T^2 \subset T^3$ under which Q is invariant. Let $\pi: \text{Lie}(T^3)^* \rightarrow \text{Lie}(T^2)^*$ be the linear map dual to the Lie algebra inclusion for the subtorus. Sketch the image of Q under $\pi \circ \mu$. Deduce that Q is symplectomorphic to $S^2 \times S^2$.

Exercise 3.5.9. More generally, let Δ be a compact polytope in \mathbf{R}^n whose vertices are in the integer lattice. To each lattice point $p_i = (p_i^1, \dots, p_i^n) \in \Delta$, $i = 0, \dots, N$, consider the monomial $z^{p_i} =$

$z_1^{p_1} \cdots z_n^{p_n}$. Let X_Δ denote the Zariski-closure of the image of

$$F: (\mathbf{C}^*)^n \rightarrow \mathbf{CP}^N, \quad F(z_1, \dots, z_n) = [z^{p_0} : \cdots : z^{p_N}].$$

Check that each point of the form $[0 : \cdots : 0 : 1 : 0 : \cdots : 0]$ is in X_Δ . Let $\pi: \mathbf{R}^N \rightarrow \mathbf{R}^n$ be the projection whose matrix is

$$\begin{pmatrix} p_0^1 & p_0^1 & \cdots & p_N^1 \\ p_0^2 & \ddots & & p_N^2 \\ \vdots & & \ddots & \vdots \\ p_0^n & \cdots & \cdots & p_N^n \end{pmatrix}.$$

If $\mu: \mathbf{CP}^N \rightarrow \mathbf{R}^N$ is the moment map for the standard T^N -action, show that the image of $\pi \circ \mu$ is the polytope Δ . You may use the fact that the moment polytope is the convex hull of its vertices.

Exercise 3.5.10. Apply the algorithm from Exercise 3.5.9 to the polytope Δ with vertices $(0, 0)$, $(0, 1)$, $(2, 1)$ (this contains four lattice points). Show that X_Δ is a cone in \mathbf{CP}^3 on a smooth conic curve in \mathbf{CP}^2 . Identify which point in the polytope is the image of the singular point. Identify which cyclic quotient singularity this is using Exercise 3.5.2. Using Lemma 3.3.9, find the self-intersection of the sphere living over the edge which avoids the singular point.

Chapter 4

Focus-focus singularities

In this chapter, we begin by discussing what happens when there are no global action-angle coordinates. We will see that the image of the Hamiltonian system inherits a natural *integral affine structure* (different from the one it already has as a subset of \mathbf{R}^n). We will study this integral affine structure in the case where our Hamiltonian system exhibits a particular class of nondegenerate singularities called *focus-focus singularities*.

4.1 Flux map

There is a more geometric way to characterise the action coordinates. Let $H: X \rightarrow \mathbf{R}^n$ be an integrable Hamiltonian system. We assume

for simplicity¹ that $\omega = d\lambda$ for some 1-form λ . Let $B \subset H(X)$ denote the set of regular values of H .

Consider the local system $\xi \rightarrow B$ whose fibre over b is the abelian group $H_1(H^{-1}(b); \mathbf{Z}) \cong \mathbf{Z}^n$. Let $p: \tilde{B} \rightarrow B$ be the universal cover and let $\tilde{\xi} = p^*\xi$. Since \tilde{B} is simply-connected, $\tilde{\xi}$ is trivial. Let c_1, \dots, c_n be a \mathbf{Z} -basis of continuous sections of $\tilde{\xi} \rightarrow \tilde{B}$.

Definition 4.1.1 (Flux map). The *flux map* is defined to be the map $I: \tilde{B} \rightarrow \mathbf{R}^n$ given by

$$I(\tilde{b}) = (I_1(\tilde{b}), \dots, I_n(\tilde{b})) := \left(\frac{1}{2\pi} \int_{c_1(\tilde{b})} \lambda, \dots, \frac{1}{2\pi} \int_{c_n(\tilde{b})} \lambda \right).$$

Lemma 4.1.2 (Flux map = action coordinates). *Suppose that $\tilde{U} \subset \tilde{B}$ and $U \subset B$ are open subsets such that $p|_{\tilde{U}}: \tilde{U} \rightarrow U$ is a diffeomorphism. Then $I \circ (p|_{\tilde{U}})^{-1}: U \rightarrow \mathbf{R}^n$ gives action coordinates on U .*

Proof. By Corollary 2.5.4, it is sufficient to prove this for the local model $(U \times T^n, \omega_0) = \sum db_i \wedge dt_i$. In that case, we can pick $\lambda = \sum b_i dt_i$ and take c_1, \dots, c_n to be the standard basis of $H_1(T^n; \mathbf{Z})$. Then we get $I_i(b) = b_i$, which recovers the action coordinates. \square

Definition 4.1.3 (Fundamental action domain). We call $I(\tilde{U})$ a *fundamental action domain* for the Hamiltonian system.

Remark 4.1.4. If we pick a different λ' such that $d\lambda' = d\lambda$ then $\lambda - \lambda'$ is closed, so $\int_{c_i(b)} (\lambda - \lambda')$ is constant (by Stokes's theorem) and the flux map changes by an additive constant. If we pick a different \mathbf{Z} -basis (c'_1, \dots, c'_n) then we can express the new integrals as a \mathbf{Z} -linear combination of I_1, \dots, I_n . This means that the flux map is determined up to a transformation of the form $x \mapsto Ax + c$ where $A \in GL(n, \mathbf{Z})$ and $c \in \mathbf{R}^n$. Such transformations are called *integral affine transformations*.

¹You might like to think about how to remove this assumption using Stokes's theorem.

Definition 4.1.5. An *integral affine structure* on an n -manifold is an atlas whose transition functions are integral affine transformations, that is transformations of the form $x \mapsto Ax + b$ with $A \in GL(n, \mathbf{Z})$ and $b \in \mathbf{R}^n$.

Corollary 4.1.6. *The space B inherits a canonical integral affine structure.*

Proof. We can pull back the integral affine structure from \mathbf{R}^n along I to get an integral affine structure on \tilde{B} . Next, we show that this integral affine structure on \tilde{B} descends to one on B , by showing that it is invariant under the action² of deck transformations. If $g: \tilde{B} \rightarrow \tilde{B}$ is a deck transformation of the cover p then $c_1(\tilde{b}), \dots, c_n(\tilde{b})$ and $c_1(\tilde{b}g), \dots, c_n(\tilde{b}g)$ are both \mathbf{Z} -bases for the \mathbf{Z} -module $H_1(H^{-1}(p(\tilde{b})); \mathbf{Z})$ and therefore they are related by some change-of-basis matrix $M(g) \in GL(n, \mathbf{Z})$. This implies that $I(\tilde{b}g) = M(g)I(\tilde{b})$. Since $M(g)$ is an integral affine transformation, this shows that the integral affine structure descends to the quotient B . \square

Note that $M(g_1g_2) = M(g_1)M(g_2)$ because we wrote the action of the deck group on the right. Indeed, $M: \pi_1(B) \rightarrow GL(n, \mathbf{Z})$ is the monodromy of the local system $\xi \rightarrow A$.

Definition 4.1.7. We call $M: \pi_1(B) \rightarrow GL(n, \mathbf{Z})$ the *affine monodromy* in what follows

Remark 4.1.8. The manifold B can be reconstructed in the usual way as a quotient of a closed fundamental domain for the universal cover $\tilde{B} \rightarrow B$ where the identifications are made using deck transformations. If we wish to reconstruct the integral affine structure on B then we use a fundamental action domain and the identifications are made using the integral affine transformations $M(g)$ corresponding to deck transformations g .

Remark 4.1.9. Given any integral affine manifold B , there is a *developing map*, that is a (globally-defined) local diffeomorphism $I: \tilde{B} \rightarrow$

²We consider the deck group acting on the right.

\mathbf{R}^n from the universal cover into Euclidean space such that the integral affine structure inherited by \tilde{B} from the covering map agrees with the pullback of the integral affine structure along the developing map. In our context, the flux map is the developing map.

Remark 4.1.10. Note that B already has an integral affine structure as it is an open subset of \mathbf{R}^n . This does not agree with the integral affine structure constructed in Corollary 4.1.6 unless H_1, \dots, H_n are already action coordinates.

Remark 4.1.11. Suppose that H has some toric singularities. It is a result of Eliasson [6] and Dufour-Molino [4] that the integral affine structure extends over the set $H(D)$ where D is the locus of toric singularities. The result is an integral affine manifold with boundary and corners. This may not be a convex polytope, and we will see examples where it is not, but the boundary components are nonetheless rational affine linear subspaces and the boundary and corners are Delzant (which is a local condition).

4.2 Focus-focus singularities

We now allow our Hamiltonian system to have singularities of a new sort (*focus-focus singularities*) and compute the action coordinates in a neighbourhood of a singular fibre. The affine monodromy will turn out to be nontrivial.

Example 4.2.1 (Local model). Consider the following pair of Poisson commuting Hamiltonians on $(\mathbf{R}^4, dp_1 \wedge dq_1 + dp_2 \wedge dq_2)$,

$$F_1 = -p_1q_1 - p_2q_2, \quad F_2 = p_2q_1 - p_1q_2.$$

If we introduce complex coordinates³ $p = p_1 + ip_2$, $q = q_1 + iq_2$ then $F := F_1 + iF_2 = -\bar{p}q$. The Hamiltonian F_1 generates the \mathbf{R} -action

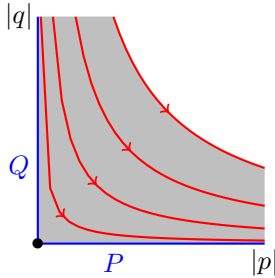
³These complex coordinates are not supposed to be compatible with ω , indeed the p -plane and q -plane are both Lagrangian.

$(p, q) \mapsto (e^t p, e^{-t} q)$. The Hamiltonian F_2 generates the circle action $(p, q) \mapsto (e^{it} p, e^{it} q)$. The orbits of the resulting $\mathbf{R} \times S^1$ -action are: the origin (fixed point); the Lagrangian cylinders $P := \{(p, 0) : p \neq 0\}$ and $Q := \{(0, q) : q \neq 0\}$; and the Lagrangian cylinders $\{(p, q) : \bar{p}q = c\}$ for $c \in \mathbf{C} \setminus \{0\}$.

The diagram below represents the projection of \mathbf{R}^4 to \mathbf{R}^2 via

$$(p_1, p_2, q_1, q_2) \mapsto (|p|, |q|);$$

the projections of the $\phi_t^{F_1}$ -flowlines are the red hyperbolae ($\phi_t^{F_2}$ -flowlines project to points). The Lagrangian cylinders P and Q are shown in blue, the fixed point is marked in black.



Definition 4.2.2. A *focus-focus chart* for an integrable Hamiltonian system $H: X \rightarrow \mathbf{R}^2$ is a pair of embeddings $E: U \rightarrow X$ and $e: V \rightarrow \mathbf{R}^2$ where $U \subset \mathbf{R}^4$ is a neighbourhood of the origin, $V = F(U)$ (where F is the Hamiltonian system in Example 4.2.1), $E^*\omega = \sum dp_i \wedge dq_i$ and $H \circ E = e \circ F$. We say that $H: X \rightarrow \mathbf{R}^2$ has a *focus-focus singularity* at $x \in X$ if there is a focus-focus chart (E, e) with $E(0) = x$.

Remark 4.2.3. This is not the standard definition of a focus-focus singularity: usually you only specify that H has a critical point at x and that the Hessian of H at x agrees with the Hessian of F at 0 . The fact that these two definitions are equivalent is a special case of

Eliasson's normal form theorem for non-degenerate singularities of Hamiltonian systems. For a proof of this special case, see [3].

Lemma 4.2.4. *Let $H: X \rightarrow \mathbf{R}^2$ be an integrable Hamiltonian system with a focus-focus singularity x over the origin and no other critical points. The fibre $H^{-1}(0)$ is homeomorphic to a pinched torus.*

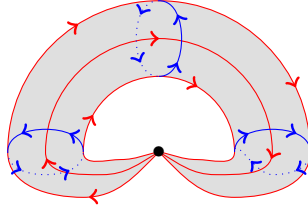
Proof. The fibre $H^{-1}(0)$ is a union of orbits $O_0 \cup O_1 \cup \dots \cup O_m$ of the \mathbf{R}^2 -action. One of these orbits (say O_0) is the fixed point x . The complement $H^{-1}(0) \setminus \{x\}$ is a 2-manifold as x is the only critical point of H ; the other orbits O_1, \dots, O_m are codimension zero submanifolds, homeomorphic to one of T^2 , $\mathbf{R} \times S^1$, or \mathbf{R}^2 if the stabiliser is isomorphic to \mathbf{Z}^2 , \mathbf{Z} or the trivial group respectively. Since these are codimension zero submanifolds without boundary, they are open, so O_1, \dots, O_m are connected components of $H^{-1}(0)$. The closure of O_k is therefore either O_k or $O_k \cup \{x\}$. There are at most two orbits whose closure contains x , as we see by looking in a focus-focus chart (E, e) centred at x : the orbit containing $E(P)$ and the orbit containing $E(Q)$.

Let (E, e) be a focus-focus chart centred at x . Let O_1 be the orbit containing $E(P)$. For each $(p, 0) \in P$, we have $\lim_{t \rightarrow -\infty} \phi_t^{H_1}(E(p, 0)) = \lim_{t \rightarrow -\infty} E(e^t p, 0) = x$. Since the fibres of H are compact, the sequence $\phi_t^{H_1}(E(p, 0))$ has a convergent subsequence whose limit lies in $H^{-1}(0)$. This limit point cannot be a regular point for H : a regular point of H has a neighbourhood

then $O_1 \cong \mathbf{R} \times S^1$. If O_1 also contains $E(Q)$ then $O_0 \cup O_1$ is a pinched torus and there can be no further orbits as the fibre would be disconnected. Otherwise, let $O_2 \cong \mathbf{R} \times S^1$ be the orbit containing $E(Q)$. Then the union $O_0 \cup O_1 \cup O_2$ is homeomorphic to a union of two planes, hence noncompact, and the further union $O_0 \cup \dots \cup O_m$ is still noncompact, which is a contradiction. Therefore $H^{-1}(0) = O_0 \cup O_1$ where $O_1 \cong \mathbf{R} \times S^1$. \square

The figure below shows a pinched torus fibre containing a focus-focus

singularity. The $\phi_t^{H_1}$ -flowlines are shown in red, the $\phi_t^{H_2}$ -flowlines in blue, and the fixed point is shown in black.



Remark 4.2.5. The same argument generalises to show that if $H^{-1}(0)$ contains $m > 1$ focus-focus singularities then it will form a cyclic chain of Lagrangian spheres, each intersecting the next transversely at a single focus-focus point (or, if $m = 2$, two spheres intersecting transversely at two points).

4.3 Action coordinates

Let $H: X \rightarrow \mathbf{R}^2$ be an integrable Hamiltonian system with a focus-focus singularity x over the origin and no other critical points. Let $E: U \rightarrow X$, $e: V \rightarrow \mathbf{R}^2$ be a focus-focus chart centred at x and, by shrinking U and V if necessary, assume that $V = \{b \in \mathbf{R}^2 : |b| < \epsilon\}$ for some $\epsilon > 0$; write $B := V \setminus \{0\}$ for the set of regular values of H . By Corollary 4.1.6, B inherits an integral affine structure, coming from action coordinates on the universal cover \tilde{B} . The next theorem identifies these action coordinates.

Theorem 4.3.1 (San Vu Ngoc). *The action map $\tilde{B} \rightarrow \mathbf{R}^2$ has the form*

$$\left(\frac{1}{2\pi} (Tb_1 + S(b) + b_2\theta - b_1(\log r - 1)), b_2 \right),$$

where $b = b_1 + ib_2 = re^{i\theta}$ is the local coordinate on B , $S(b)$ is a smooth function and T is a constant.

Proof. Recall that $F: U \rightarrow V$ denotes the model Hamiltonian from Example 4.2.1. Observe that $\sigma_1: V \rightarrow \mathbf{R}^4$, $\sigma_1(b) = (-\bar{b}, 1)$ is a Lagrangian section of F which intersects the branch Q of $F^{-1}(0)$. In the proof of Lemma 4.2.4, we saw that the branch $E(P)$ is part of the same \mathbf{R}^2 -orbit as the branch $E(Q)$. Therefore, if we flow $E(\sigma_1(0))$ for sufficiently long using $\phi_{-t}^{H_1}$, we will reach a point in $E(P)$. Indeed, by shrinking V , we can assume that $E(\sigma_1(V))$ is contained in $E(U)$. This gives a Lagrangian section of H of the form $e \circ \sigma_2$, where, $\sigma_2: V \rightarrow \mathbf{R}^4$ is a Lagrangian section of F which intersects the branch P of $F^{-1}(0)$ (Figure 4.1).

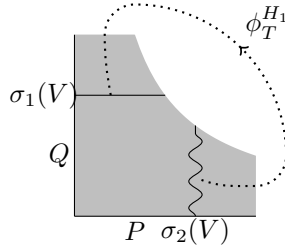


Figure 4.1: For sufficiently small V there exists $T \in \mathbf{R}$ such that $\phi_{-T}^{H_1}(\sigma_1(V))$ is a section in the focus-focus chart, intersecting the branch P of the singular fibre.

Suppose that $\sigma_2(b) = (-\alpha(b), \beta(b))$. Then, since $b = F(-\bar{b}, 1)$, we have $\bar{\alpha}(b)\beta(b) = F(-\alpha(b), \beta(b)) = F(\phi_{-T}^{H_1}(-\bar{b}, 1)) = F(-\bar{b}, 1) = b$. Over $B = V \setminus \{0\}$, let us write $\alpha(b) = \exp(S_1(b) + iS_2(b))$ for some functions S_1, S_2 . Then $\beta(b) = be^{-S_1(b) + iS_2(b)}$. Note that

$$\sigma_2(b) = \phi_{S_1(b) - \ln |b|}^{F_1} \phi_{S_2(b) + \arg(b)}^{F_2}(\sigma_1(b)).$$

Since $\phi_T^{F_1}(\sigma_1(b)) = \sigma_2(b)$ by definition, we have

$$\sigma_1(b) = \phi_{T + S_1(b) - \ln |b|}^{H_1} \phi_{S_2(b) + \arg(b)}^{H_2}(\sigma_1(b)),$$

so $\phi_{T+S_1(b)-\ln|b|}^{F_1} \phi_{S_2(b)+\arg(b)}^{F_2} = id$ on the complement of the fibre $H^{-1}(0)$. Since $\phi_{2\pi}^{F_2} = id$, we see that the period lattice is

$$\Lambda_b = \mathbf{Z} \begin{pmatrix} T + S_1(b) - \ln|b| \\ S_2(b) + \arg(b) \end{pmatrix} \oplus \mathbf{Z} \begin{pmatrix} 0 \\ 2\pi \end{pmatrix}.$$

To find the action coordinates (f_1, f_2) , we need to solve

$$\begin{pmatrix} \frac{\partial f_1}{\partial b_1} & \frac{\partial f_1}{\partial b_2} \\ \frac{\partial f_2}{\partial b_1} & \frac{\partial f_2}{\partial b_2} \end{pmatrix} = \begin{pmatrix} \frac{1}{2\pi}(T + S_1(b) - \ln|b|) & \frac{1}{2\pi}(S_2(b) + \arg(b)) \\ 0 & 1 \end{pmatrix}.$$

The integrability condition Equation (2.2) (which is equivalent to σ_2 being a Lagrangian section) becomes

$$\frac{\partial S_1}{\partial b_2} = \frac{\partial S_2}{\partial b_1}, \quad (4.1)$$

which holds if and only if $S_1 = \frac{\partial S}{\partial b_1}$ and $S_2 = \frac{\partial S}{\partial b_2}$ for some function $S: \mathbf{R}^2 \rightarrow \mathbf{R}$.

Provided the integrability condition is satisfied, the solution is given by $f_1(b) = \frac{1}{2\pi}(Tb_1 + S(b) + \theta b_2 - b_1(\log r - 1))$, $f_2(b) = b_2$, where $b = b_1 + ib_2 = re^{i\theta}$.

□

Remark 4.3.2. In fact, any such S arises as we will show in the next section. Moreover, Ngoc [11] showed⁴ that the germ of S near the origin is unchanged by any symplectomorphism of the system preserving the foliation by fibres of π . We will write $(S)^\infty$ for the Ngoc invariant of a focus-focus singularity.

⁴There is a subtlety here: the germ of S can depend on the choice of focus-focus chart. This is a finite ambiguity, overlooked in Ngoc's original paper, and is discussed in [9, Section 4.3]: the actual Ngoc invariant is an equivalence class of germs under an action of the Klein 4-group.

Remark 4.3.3. The action map does not descend to B : it depends explicitly on the multivalued function θ . In fact, if one moves once around the focus-focus singularity in the base of the Lagrangian bundle then the action map is changed by the application of the matrix

$$\begin{pmatrix} 1 & 1 \\ 0 & 1 \end{pmatrix}.$$

As discussed in the proof of Corollary 4.1.6, this is therefore the monodromy of the period lattice.

Remark 4.3.4. The action map has a well-defined limit point as $r \rightarrow 0$. We call this limit point the *base node* of the focus-focus singularity.

We conclude this section with some fundamental action domains for different choices of fundamental domain for the covering map $\tilde{B} \rightarrow B$ (for the choice $S \equiv 0$). We include the images under the action map of contours of constant r (in blue) and constant θ (in red).

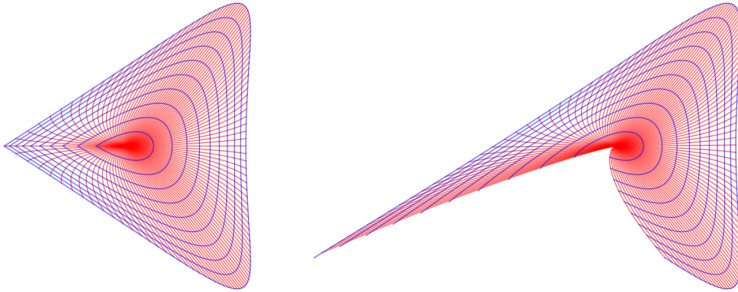


Figure 4.2: In left-hand figure, we see the the image of the fundamental domain $\{\theta \in [-\pi, \pi)\}$, in the right the image of the fundamental domain $\{\theta \in [-5\pi/7, 9\pi/7)\}$. The fact that the plot on the right does not “close up” is because of the monodromy: the image of the radius $\theta = -5\pi/7$ and the image of the radius $\theta = 9\pi/7$ are related by the monodromy matrix. The fact that the first plot does “close up” is because the line $\theta = \pi$ is an eigendirection for the monodromy matrix.

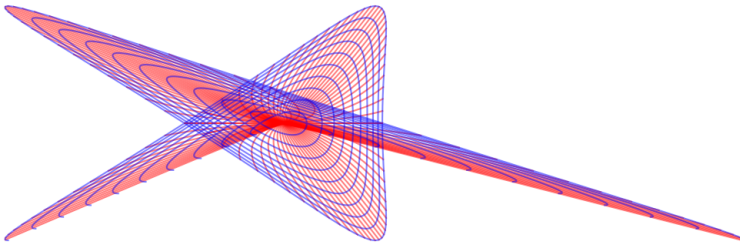


Figure 4.3: In the third figure, we see the image of two fundamental domains $\{\theta \in [-5\pi/2, 3\pi/2)\}$, related to one another by the action of the monodromy matrix⁵.

⁵Anyone who has compulsively traced out the spiral of a raffia mat cannot fail to be moved by this image.

4.4 Model neighbourhoods

We now present a construction due to Ngoc which, given a function $S: \mathbf{R}^2 \rightarrow \mathbf{R}$, produces a Hamiltonian system $H_S: X_S \rightarrow \mathbf{R}^2$ with a focus-focus singularity whose Ngoc invariant is $(S)^\infty$. We will write $S_i = \frac{\partial S}{\partial b_i}$, $i = 1, 2$.

Take the subset $X := \{(p, q) \in \mathbf{R}^4 : |\bar{p}q| < \epsilon\}$ equipped with the Hamiltonian system F from Example 4.2.1. We will construct two Liouville coordinate systems on different regions of this space.

We use the Lagrangian section $\sigma_1(b) = (-\bar{b}, 1)$ and the coordinates (b_1, b_2) on \mathbf{R}^2 to construct Liouville coordinates in a neighbourhood of the subset $\{(p, q) \in \mathbf{R}^4 : |q| = 1\}$. In other words, we use the symplectic embedding $\Psi_1: (b_1, b_2, t_1, t_2) \mapsto \phi_{t_1}^{F_1} \phi_{t_2}^{F_2}(\sigma_1(b))$, $0 \leq t_1 < \delta$, $t_2 \in [0, 2\pi)$. That is

$$p = e^{t_1 + it_2 \bar{b}}, \quad q = e^{-t_1 + it_2}.$$

We use the Lagrangian section $\sigma_2(b) = (-e^{S_1(b) + iS_2(b)}, be^{-S_1(b) + iS_2(b)})$ and the coordinates (b_1, b_2) on \mathbf{R}^2 to construct Liouville coordinates in a neighbourhood of the subset $\{(p, q) : |p| = e^{S_1(\bar{p}q)}\}$. In other words, we use the symplectic embedding $\Psi_2: (b_1, b_2, t_1, t_2) \mapsto \phi_{t_1}^{F_1} \phi_{t_2}^{F_2}(\sigma_2(b))$, $0 \leq t_1 < \delta$, $t_2 \in [0, 2\pi)$.

Let $X' = \{(p, q) \in \mathbf{R}^4 : |\bar{p}q| < \epsilon, |q| \leq 1, |p| \leq e^{S_1(\bar{p}q)}\}$ and let X_S be the quotient $X_S := X' / \sim$, where \sim identifies $\Psi_1(b, t) \sim \Psi_2(b, t)$. Since the domains of Ψ_1 and Ψ_2 are identical and since Ψ_1, Ψ_2 are symplectomorphisms, the symplectic form on X descends to this quotient. By construction, the map $H: X \rightarrow \mathbf{R}^2$, $\pi(p, q) = \bar{p}q$ descends to the quotient and produces the Hamiltonian system H_S we want. Also by construction, the Ngoc invariant is $(S)^\infty$.

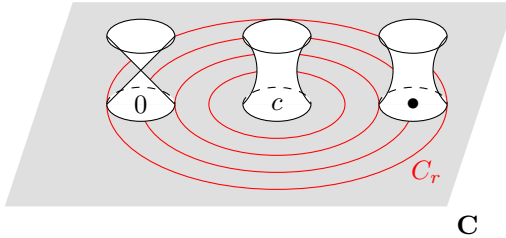
Remark 4.4.1. In our earlier exposition, we flowed using $\phi_{-T}^{H_1}$ to relate the Lagrangian sections σ_1 and σ_2 ; in this model, we have $T = 0$. Note that T can always be absorbed into a Tb_1 term in S .

4.5 The Auroux system

Like many people, I first learned of the following example from the wonderful expository article [2] on mirror symmetry for Fano varieties by D. Auroux, where it serves to illustrate the wall-crossing phenomenon for discs.

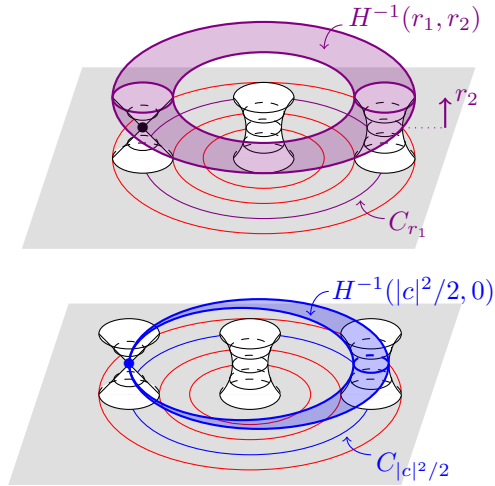
Example 4.5.1 (Auroux system). Fix a real number $c > 0$. Consider the Hamiltonians $(H_1, H_2): \mathbf{C}^2 \rightarrow \mathbf{R}^2$ defined by $H_1(z_1, z_2) = \frac{1}{2}|z_1 z_2 - c|^2$ and $H_2(z_1, z_2) = \frac{1}{2}(|z_1|^2 - |z_2|^2)$. The flow of H_2 is $\phi_t^{H_2}(z_1, z_2) = (e^{it} z_1, e^{-it} z_2)$. This shows that $\{H_1, H_2\} = 0$, because H_1 is constant along the flow of H_2 (see Lemma 2.2.8). The flow of H_1 is harder to compute. We can nonetheless understand the orbits of this system geometrically.

Consider the holomorphic map $\pi: \mathbf{C}^2 \rightarrow \mathbf{C}$, $\pi(z_1, z_2) = z_1 z_2$. This is a conic fibration: the fibres $\pi^{-1}(p)$ are smooth conics except $\pi^{-1}(0)$ which is a singular conic (union of the z_1 - and z_2 -axes).



The Hamiltonian H_1 measures the squared distance in \mathbf{C} from $z_1 z_2$ to some fixed point c . The level set $H_1^{-1}(r)$ is therefore the union of all conics living over a circle C_r of radius $\sqrt{2r}$ centred at c (the red circles in the figure). The restriction of H_2 to each conic can be visualised as a “height function” whose level sets are circles as shown below. The level set $H^{-1}(r_1, r_2)$ is therefore the union of all circles of height r_2 in conics living over the circle C_r . These level sets are clearly tori, except for the level set $(\frac{1}{2}|c|^2, 0)$, which is a

pinched torus.



It is an exercise to check that this system has a focus-focus singularity at $(0, 0)$. It also has toric singularities along the conic $z_1 z_2 = c$.

4.5.1 Fundamental action domain

Lemma 4.5.2. *There is a fundamental action domain for this system of the form*

$$\{(x_1, x_2) : 0 \leq x_1 \leq f(x_2)\} \setminus \{(x_1, 0) : x_1 \geq m\}$$

for some function $f: \mathbf{R} \rightarrow (0, \infty)$ and some number $m > 0$ (see Figure 4.4). The affine monodromy, on crossing the branch cut $\{(x_1, 0) : x_1 \geq m\}$, is $\begin{pmatrix} 1 & 1 \\ 0 & 1 \end{pmatrix}$.

Remark 4.5.3. Finding f and m precisely along with the actual map from \tilde{U} to this domain is a nontrivial task. Technically, we should



Figure 4.4: The fundamental action domain from Lemma 4.5.2.

also specify whether the monodromy is to be applied when we cross the branch cut clockwise or anticlockwise around the singularity; in this case we can always postcompose with a reflection $x_2 \mapsto -x_2$ to switch these two, so it is not important.

Proof of Lemma 4.5.2. The image $H(\mathbf{C}^2)$ is the closed right half-plane: H_1 is always positive and H_2 can take on any value. The vertical boundary of the half-plane is the image of the toric boundary (the conic $z_1 z_2 = c$). The point $p = (\frac{1}{2}|c|^2, 0)$ is the image of the focus-focus singularity $(0, 0)$ and $B = H(\mathbf{C}^2) \setminus \{p\}$.

The Hamiltonian H_2 gives a 2π -periodic flow, so the change of coordinates of \mathbf{R}^2 which gives action coordinates has the form $(x_1, x_2) \mapsto (G_1(x_1, x_2), x_2)$ for some (multiply-valued) function G_1 . In particular, the monodromy of the integral affine structure around the focus-focus singularity simply shifts amongst the branches of G_1 , so has the form $\begin{pmatrix} 1 & 1 \\ 0 & 1 \end{pmatrix}$. We may make a branch cut along the line $R = \{(x_1, 0) : x_1 > \frac{1}{2}|c|^2\}$ to get a simply-connected open set $U = B \setminus R$ and pick a fundamental domain \tilde{U} lying over U in the universal cover $p: \tilde{B} \rightarrow B$.

We first compute the image $\{(G_1(0, x_2), x_2) : x_2 \in \mathbf{R}\}$ of the line $0 \times \mathbf{R}$ under the action coordinates. We know by Remark 4.1.11 that this will be a straight line S with rational slope. Moreover, there is a visible Lagrangian disc $\{(z, \bar{z}) : |z|^2 \leq c\}$ with boundary on $z_1 z_2 = c$; this visible disc lives over the horizontal line segment

$\{(x_1, 0) : x_1 \leq |c|^2/2\}$ under the map H and hence over a horizontal line segment $\{(G_1(x_1, 0), 0) : x_1 \leq |c|^2/2\}$ in the image of action coordinates. Since this is a disc, not a pinwheel core, comparison with the local models from Example 3.4.6 shows that the line S must slope $1/n$ for some integer n . In particular, postcomposing action coordinates with an integral affine shear $\begin{pmatrix} 1 & -n \\ 0 & 1 \end{pmatrix}$, we get that S is vertical (we always have the freedom to postcompose our action coordinates with an integral affine transformation). Now it is clear that the fundamental action domain has the required form, where $f(x_2) = \sup_{x_1 \in [0, \infty)} G_1(x_1, x_2)$ and $m = G_1(p)$. \square

4.5.2 Different branch cuts

We can always pick a different simply-connected domain $U \subset B$ to get well-defined action coordinates, as illustrated in Figure 4.2. This will not in general “close-up”, and there will be two branch cuts related by the affine monodromy. We plot some of the associated pictures below as the branch cut under goes a full rotation. It is important to emphasise that all of these are fundamental action domains for the *same* Hamiltonian system on the *same* manifold; they differ only in the choice of a fundamental domain for the covering space $\tilde{B} \rightarrow B$.

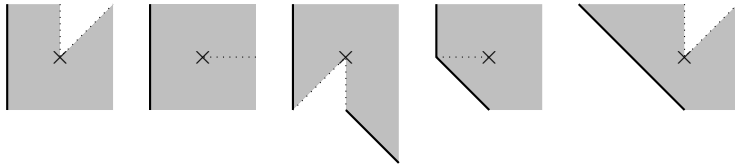


Figure 4.5: The Auroux system seen with different branch cuts; as we move from left to right in the figure, we see the branch cut rotate by 360 degrees. The final picture is related to the first by the affine monodromy.

Remark 4.5.4. In some of these pictures, the toric boundary appears “broken”. This is an artefact of the fact that it intersects the branch cut: the two segments of the toric boundary are related by the affine monodromy and therefore form one straight line in the integral affine structure. If you want to check this, I have chosen the affine monodromy to be $\begin{pmatrix} 1 & -1 \\ 0 & 1 \end{pmatrix}$ as you cross the branch cut *anticlockwise*, so, for example in the fourth picture from the left, the tangent vector $\begin{pmatrix} 0 \\ -1 \end{pmatrix}$ to the line above the branch cut gets sent to $\begin{pmatrix} 1 & -1 \\ 0 & 1 \end{pmatrix} \begin{pmatrix} 0 \\ -1 \end{pmatrix} = \begin{pmatrix} 1 \\ -1 \end{pmatrix}$ below the branch cut, which is tangent to the continuation of the boundary.

Moreover, we can apply an integral affine transformation to any of these diagrams. Applying the matrix $\begin{pmatrix} 1 & 0 \\ 1 & 1 \end{pmatrix}$ to the fourth diagram from the left yields Figure 4.6 which will be important in the next chapter. The point is that away from the branch cut, the affine manifold looks like the standard Delzant corner. We will see that this means we can always “implant” this local Hamiltonian system whenever we have a polygon with a standard Delzant corner, an operation known as a *nodal trade*.

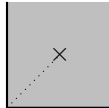


Figure 4.6: Another fundamental action domain for the Auroux system.

4.5.3 Visible Lagrangians

In our analysis of the Auroux system, the visible Lagrangian disc $\{(z, \bar{z}) : |z|^2 \leq c\}$ played an important role. The following result tells us that we can always find such a disc near a focus-focus singularity.

Lemma 4.5.5. *Let $H : X \rightarrow \mathbf{R}^2$ be an integrable Hamiltonian system with a focus-focus singularity at $x \in X$, let B be the set of regular values and \tilde{B} its universal cover, and let $I : \tilde{B} \rightarrow \mathbf{R}^2$ be the developing map for the integral affine structure on B coming from action coordinates. Let $p \in \mathbf{R}^2$ be the base node of x . Suppose that ℓ is a straight ray in \mathbf{R}^2 emanating from b and that ℓ points in an eigendirection for the affine monodromy around the singularity. Then there is a visible Lagrangian disc living over ℓ .*

Proof. In the focus-focus chart we can simply use the Lagrangian disc $q = p$, which satisfies $F(p, p) = -\bar{p}p$, so this lives over the negative x_1 -axis ($x_2 = 0$). By Theorem 4.3.1, passing to action coordinates preserves this line, which is an eigenray of the affine monodromy. \square

Definition 4.5.6. By analogy with the (slightly different⁶) situation in Picard-Lefschetz theory, this visible Lagrangian disc is called the *vanishing thimble* for the focus-focus singularity, and its intersection with any fibre over the ray ℓ is a loop called the *vanishing cycle*.

4.6 Symington's theorem

We now present an argument of Symington [?] which tells us that, although the Ngoc models $H_{S_0} : X_{S_0} \rightarrow \mathbf{R}^2$, $H_{S_1} : X_{S_1} \rightarrow \mathbf{R}^2$ with

⁶In Picard-Lefschetz theory, we have a *holomorphic* fibration instead of a Lagrangian fibration, but the thimble is still a Lagrangian disc.

$(S_0)^\infty \neq (S_1)^\infty$ are not symplectomorphic via a fibred symplectomorphism, there is nonetheless a symplectomorphism $X_{S_0} \rightarrow X_{S_1}$ which is fibred outside a compact set.

Theorem 4.6.1 (Symington). *Let $S_0: \mathbf{R}^2 \rightarrow \mathbf{R}$ and $S_1: \mathbf{R}^2 \rightarrow \mathbf{R}$ be smooth functions which coincide on the complement of a small disc D centred at the origin and let $H_{S_0}: X_{S_0} \rightarrow \mathbf{R}^2$ and $H_{S_1}: X_{S_1} \rightarrow \mathbf{R}^2$ be the corresponding Ngoc models. Then there is a symplectomorphism $\varphi: X_{S_0} \rightarrow X_{S_1}$ which restricts to a fibred symplectomorphism $H_{S_0}^{-1}(\mathbf{R}^2 \setminus D) \rightarrow H_{S_1}^{-1}(\mathbf{R}^2 \setminus D)$.*

Proof. Pick a family S_t interpolating between S_0 and S_1 such that $S_t|_{\mathbf{R}^2 \setminus D} = S_0|_{\mathbf{R}^2 \setminus D}$. Consider the family of symplectic manifolds X_{S_t} ; the subsets $H_{S_t}^{-1}(\mathbf{R}^2 \setminus D)$ are canonically symplectomorphic. There is a diffeomorphism $\varphi_t: X_{S_0} \rightarrow X_{S_t}$ which extends this canonical symplectomorphism, so we obtain a family of symplectic forms $\varphi_t^* \omega_{S_t}$ on X_{S_0} . These are all exact forms and the derivative $\frac{d}{dt} \varphi_t^* \omega_{S_t}$ vanishes outside $H_{S_0}^{-1}(\mathbf{R}^2 \setminus D)$. Therefore, by Moser's trick (see exercises), there are diffeomorphisms $\phi_t: X_{S_0} \rightarrow X_{S_0}$, equal to the identity outside $H_{S_0}^{-1}(\mathbf{R}^2 \setminus D)$, such that $\phi_t^* \varphi_t^* \omega_{S_t} = \omega_{S_0}$. The symplectomorphism we want is $\varphi := \varphi_1 \circ \phi_1: X_{S_0} \rightarrow X_{S_1}$. \square

4.7 Exercises

Exercise 4.7.1. Verify that the flows of the Hamiltonians F_1, F_2 from Example 4.2.1 are as claimed, and that the Hamiltonians Poisson-commute.

Exercise 4.7.2. Check that $\sigma_2(b) = (e^{S_1(b)+iS_2(b)}, be^{-S_1(b)+iS_2(b)})$ is a Lagrangian section of the focus-focus system if and only if $\frac{\partial S_1}{\partial b_2} = \frac{\partial S_2}{\partial b_1}$.

Exercise 4.7.3. Check that the Hessian of H_1 at the origin in the Auroux system at the agrees (up to a symplectic change of basis)

with that of F_1 from Example 4.2.1. Together with Remark 4.2.3, this shows that the Auroux system has a focus-focus singularity at the origin.

Exercise 4.7.4. In this exercise, we use the notation from Section 4.1, but we will allow $[\omega] \neq 0 \in H^2(X; \mathbf{R})$ and attempt to define flux coordinates. Pick a point $\tilde{b} \in \tilde{B}$. For every $\tilde{b}' \in \tilde{B}$, pick a path γ from \tilde{b} to \tilde{b}' . For each $i = 1, \dots, n$, let C_i be a cylinder living over γ so that $C_i \cap H^{-1}(p(\gamma(t)))$ is a circle in the homology class $c_i(\gamma(t))$. Let $I_i(\tilde{b}') = \int_{C_i} \omega$. Show that the resulting map $I = (I_1, \dots, I_n): \tilde{B} \rightarrow \mathbf{R}^n$ is well-defined independently of choices and that it agrees with the flux map in Definition 4.1.1 when ω is exact.

Exercise 4.7.5. Moser's trick...

Exercise 4.7.6. Take the wedge in \mathbf{R}^2 spanned by the rays $(0, 1)$ and (p, q) and let X be the associated (singular) toric manifold. By Exercise 3.5.3, we know that the preimage of the line $\{(x, 1) : x \in [0, p/q]\}$ is a lens space $L(p, q)$. By applying suitable integral affine transformations to this wedge, prove that the lens space $L(p, q + np)$ is diffeomorphic to $L(p, q)$ for all integers n . Now reflect the wedge in the vertical axis, find a matrix $M \in SL(2, \mathbf{Z})$ such that $M \begin{pmatrix} p \\ q \end{pmatrix} = \begin{pmatrix} 0 \\ 1 \end{pmatrix}$ and hence show that $L(p, q)$ is diffeomorphic to $L(p, \bar{q})$ where $q\bar{q} = -1 \pmod{p}$.

Exercise 4.7.7. Let $p(z)$ be a polynomial of degree $n + 1$ with $n + 1$ distinct roots. Let $A_n = \{(x, y, z) \in \mathbf{C}^3 : xy + p(z) = 0\}$. By considering the conic fibration $\pi: A_n \rightarrow \mathbf{C}$, $\pi(x, y, z) = z$, find integrable Hamiltonian systems $H: A_n \rightarrow \mathbf{R}^2$ with the following properties:

1. When $p(z) = z^{n+1} - 1$, a line of toric singularities and a single fibre with $n + 1$ focus-focus singularities.

2. When $p(z) = (z - 1)(z - 2) \cdots (z - (n + 1))$, a line of toric singularities and $n + 1$ focus-focus singularities whose affine monodromies are the same.

In each case, sketch a fundamental action domain for the system. Using your solution to Exercise 3.5.3, show that the noncompact end of A_n is modelled on the lens space $L(n + 1, n)$.

Exercise 4.7.8. Let p, q be coprime positive integers, $1 \leq q < p$. Consider the action of the group μ_p of p th roots of unity on the variety $A_{p-1} = \{xy + z^p = 1\}$ from Exercise 4.7.7 given by $\mu \cdot (x, y, z) = (\mu x, \mu^{-1}y, \mu^q z)$, $\mu \in \mu_p$. Check that this action is free and that $\pi(\mu \cdot (x, y, z)) = \mu\pi(x, y, z)$. Deduce that the Hamiltonian system H from Exercise 4.7.7 descends to a system $\bar{H}: B_{p,q} \rightarrow \mathbf{R}^2$ on the quotient space $B_{p,q} := A_{p-1}/\mu_p$ with a single focus-focus singularity and $H(A_{p-1}) = \bar{H}(B_{p,q})$. By mimicking Exercise 3.5.2, find a fundamental action domain for \bar{H} and show that $B_{p,q}$ contains a *Lagrangian (p, q) -pinwheel*, that is a 2-dimensional CW complex obtained by capping off a Lagrangian (p, q) -pinwheel core with a Lagrangian disc.

Exercise 4.7.9. Generalise Exercise 4.7.8 to the case where μ_p acts (by the same formula) on $\{xy + (z^p - 1)(z^p - 4) \cdots (z^p - d^2) = 0\}$.

Exercise 4.7.10. Consider the variety $X \subset \mathbf{CP}^2 \times \mathbf{CP}^2$, given in homogeneous coordinates $([a_1 : a_2 : a_3], [b_1 : b_2 : b_3])$ by $\sum a_i b_i = 0$ (this is the *flag 3-fold*). Let $Y \subset X$ be the subvariety $a_1 b_1 = a_3 b_3$. Consider the holomorphic map

$$\pi: X \setminus Y \rightarrow \mathbf{C}, \quad \pi(a, b) = \frac{a_2 b_2}{a_3 b_3 - a_1 b_1}.$$

The general fibre of this map is biholomorphic to $(\mathbf{C}^\times)^2$, but there are singular fibres over $-1, 0, 1$. Let $c < -1$ be a real number. Show that the function $H: X \setminus Y \rightarrow \mathbf{R}^3$ defined by

$$H(a, b) = \left(\frac{1}{2} \left(\frac{|a_1|^2}{|a|^2} - \frac{|b_1|^2}{|b|^2} \right), \frac{1}{2} \left(\frac{|a_3|^2}{|a|^2} - \frac{|b_3|^2}{|b|^2} \right), \frac{1}{2} |\pi(a, b) - c|^2 \right)$$

is a Lagrangian torus fibration. The singularities comprise a plane of toric singularities and three lines of focus-focus singularities⁷. Sketch the image of H . Check that the maps

$$L_{\pm}(\theta, \phi, y) = \left(\begin{array}{l} \left[e^{i\theta} \sqrt{1 \pm y} : e^{i\phi} \sqrt{2y} : \sqrt{1 \mp y} \right], \\ \left[-e^{-i\theta} \sqrt{1 \pm y} : \pm e^{-i\phi} \sqrt{2y} : \sqrt{1 \mp y} \right] \end{array} \right)$$

define two Lagrangian 3-spheres in $X \setminus Y$ and sketch their images under H . Here, we are thinking of the 3-sphere as a family of 2-tori (each having coordinates (θ, ϕ)) parametrised by $y \in [0, 1]$ such that the ϕ -circle collapses as $y \rightarrow 0$ and the θ -circle collapses as $y \rightarrow 1$.

Remark 4.7.11. These examples all come from smoothings of singularities. If we write $\frac{1}{n}(1, m)$ for the cyclic quotient singularity from Exercise 3.5.2 then:

- the A_n space from Exercise 4.7.7 is a smoothing of the A_n -singularity $\frac{1}{n+1}(1, n)$;
- the $B_{p,q}$ space from Exercise 4.7.8 is a smoothing of the *Wahl singularity* $\frac{1}{p^2}(1, pq, -1)$;
- the space from Exercise 4.7.9 is a smoothing of the singularity $\frac{1}{dp^2}(1, dpq - 1)$. These form an important class of *T-singularities* (surface singularities which admit a \mathbf{Q} -Gorenstein smoothing, see [7]);
- the space from Exercise 4.7.10 is a smoothing of the 3-fold singularity obtained by taking a cone on the surface Y , which is itself a 3-point blow-up of \mathbf{CP}^2 .

In the first three cases, note that the fundamental action domain can be obtained from the moment polygon we found in Exercise 3.5.2 by making some (collinear) branch cuts.

⁷For 6-dimensional Hamiltonian systems, with local coordinates $(p_1, p_2, p_3, q_1, q_2, q_3)$, this means that the local model is $F_1 = -p_1 q_2 - p_2 q_3$, $F_2 = p_2 q_1 - p_1 q_3$, $F_3 = p_3$.

Chapter 5

Almost toric manifolds

5.1 Lagrangian torus fibrations

It will be convenient to allow our integrable Hamiltonian systems to have targets other than \mathbf{R}^n , so we introduce some new terminology.

Definition 5.1.1. Recall that a stratification of a topological space B is a filtration

$$\emptyset =: B_{-1} \subset B_0 \subset \cdots \subset B_d \subset B_{d+1} \subset \cdots \subset B,$$

where each B_d is a closed subset such that, for each d , the d -stratum $S_d(B) := B_d \setminus B_{d-1}$ is a smooth d -dimensional manifold (possibly empty) and $B = \bigcup_{d \geq 0} B_d$. We say that B is finite-dimensional if the d -stratum is empty for sufficiently large d , and we say that B is n -dimensional if B is finite-dimensional and n is maximal such that $S_n(B)$ is nonempty (in this case we call $S_n(B)$ the *top stratum*).

We adopt the following working definition of a Lagrangian torus fibration.

Definition 5.1.2. Let (X, ω) be a $2n$ -dimensional symplectic manifold and B be an n -dimensional stratified space. A Lagrangian torus fibration $H: X \rightarrow B$ is a proper continuous map such that H is a smooth submersion over the top stratum with Lagrangian fibres and the other fibres are themselves stratified spaces with isotropic strata. We call $S_n(B)$ the *regular locus* of H and $B \setminus S_n(B)$ the *discriminant locus*.

In Exercise 2.6.10, we saw the following result:

Theorem 5.1.3. *Let $H: X \rightarrow B$ be a Lagrangian torus fibration and let $b \in B$ be a point in the top stratum. Let $U \subset B$ be an open neighbourhood of b with local coordinates (b_1, \dots, b_n) . Then the functions $H_i := b_i \circ H: X \rightarrow \mathbf{R}^n$ form an integrable Hamiltonian system. In particular, $H^{-1}(b)$ is a Lagrangian torus by the Arnol'd-Liouville theorem.*

Definition 5.1.4. An *almost toric fibration* is a Lagrangian torus fibration $H: X \rightarrow B$ on a 4-dimensional symplectic manifold such that the discriminant locus comprises a collection of 0- and 1-dimensional strata such that the smooth structure on B extends over these strata, H is smooth with respect to this extended smooth structure and has either toric or focus-focus singularities there.

5.2 Operations

5.2.1 Nodal trade

Recall from Figure 4.6 that there is an almost toric structure on \mathbf{C}^2 which admits a fundamental action domain as drawn on the left in Figure 5.1 below. The red region in the figure is integral affine equivalent to the green region in the figure on the right, which is a subset of the moment polygon for the standard torus action on

\mathbf{C}^2 . This means that the preimages of these two regions are fibred-symplectomorphic.

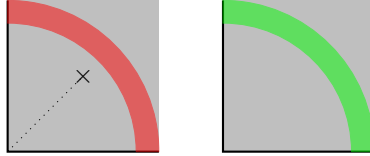


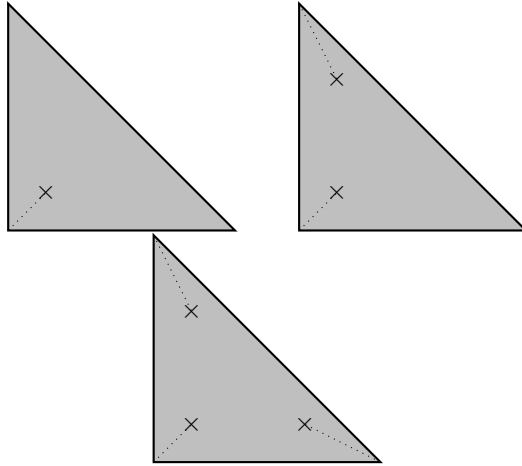
Figure 5.1: Left: A fundamental action domain for the Auroux system on \mathbf{C}^2 ; a subset is marked in red. Right: The moment image for the standard torus action on \mathbf{C}^2 ; the subset marked in green is clearly integral affine equivalent to the red subset on the right.

In particular, whenever we see a Delzant corner, we can excise it and glue in a copy of the Auroux system, using this fibred symplectomorphism to make identifications. Since the identifications are fibred, this operation yields a new Lagrangian torus fibration on the same manifold¹. In fact, there are many different operations, one for each Ngoc model, but the results are all (non-fibred) symplectomorphic to one another by Symington’s Theorem 4.6.1. We call an operation like this a *nodal trade*.

Remark 5.2.1. The toric boundary near a Delzant corner comprises two symplectic discs meeting transversally at the vertex. When you perform a nodal trade, the toric boundary becomes a symplectic annulus which is a smoothing of this pair of discs. For example, in the Auroux system this is the smoothing from $z_1 z_2 = 0$ to $z_1 z_2 = c$.

Example 5.2.2. Here are some Lagrangian torus fibrations on \mathbf{CP}^2 :

¹To see that the manifold does not change, observe that we are excising a symplectic ball and gluing in another symplectic ball with the same boundary (a contact 3-sphere). Any contactomorphism of the boundary sphere extends over the ball, because the contactomorphism group of the 3-sphere is connected [?].



The nodal trade in the lower left corner should look familiar; we call this a *standard Delzant corner*. To find the eigendirection for *any* Delzant corner p , if A is the unique integral affine transformation which maps the standard Delzant corner to p then then the eigendirection at p is $A \begin{pmatrix} 1 \\ 1 \end{pmatrix}$. For example, the top left corner is the image of the standard Delzant corner under $\begin{pmatrix} 0 & 1 \\ -1 & -1 \end{pmatrix}$, so the eigendirection is $(1, -2)$, as shown.

As noted in Remark 4.5.4, although the toric boundary looks like three line segments, every time it crosses a branch cut you have to apply the affine monodromy to its tangent vector, so the apparent breaks in the line when it crosses a branch cut are just an illusion: it is really an uninterrupted straight line in the affine structure. In the three examples above, the toric boundary comprises:

- a conic and a line (two spheres intersecting transversely at two points, one having twice the symplectic area of the other),
- a nodal cubic curve (pinched torus having symplectic area

three),

- a smooth cubic curve (torus having symplectic area three).

This should make sense: the toric boundary for the usual toric picture of \mathbf{CP}^2 comprises three lines and these configurations above are obtained by smoothing one or more intersections between these lines. Although I have used the terminology “line”, “conic”, and “cubic” from algebraic geometry, it is not clear for these new integrable Hamiltonian systems whether the toric boundary is actually a subvariety for the standard complex structure. It is, at least, a symplectic submanifold (immersed, where there are double points), and it is known that low-degree symplectic surfaces in \mathbf{CP}^2 are isotopic amongst symplectic surfaces to subvarieties, hence the abuse of terminology.

The figures on the next three pages show the image of the developing map for the integral affine structure in these three cases.

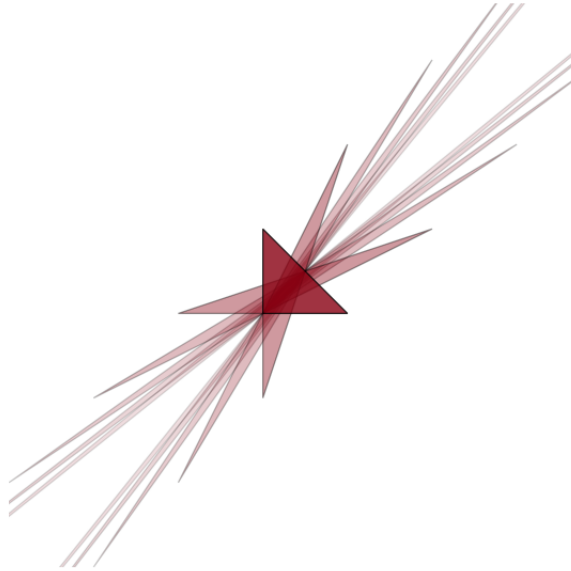


Figure 5.2: The image of the developing map for an almost toric structure on \mathbf{CP}^2 obtained from the standard moment triangle by a single nodal trade in the lower left corner.

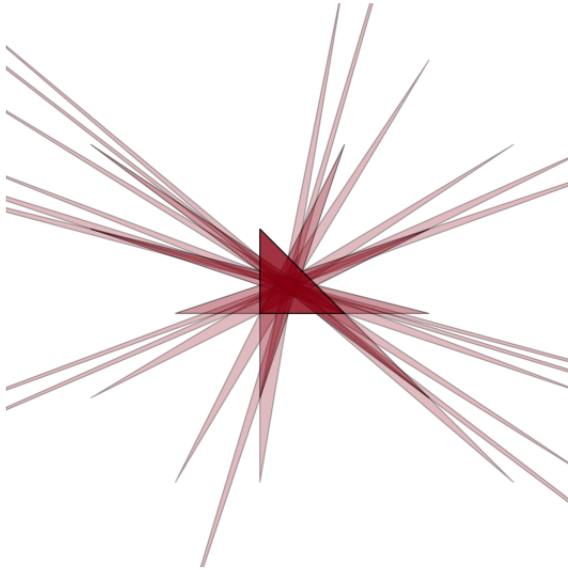


Figure 5.3: The image of the developing map for an almost toric structure on \mathbf{CP}^2 obtained from the standard moment triangle by a nodal trade in the lower left corner and a nodal trade in the lower right corner.

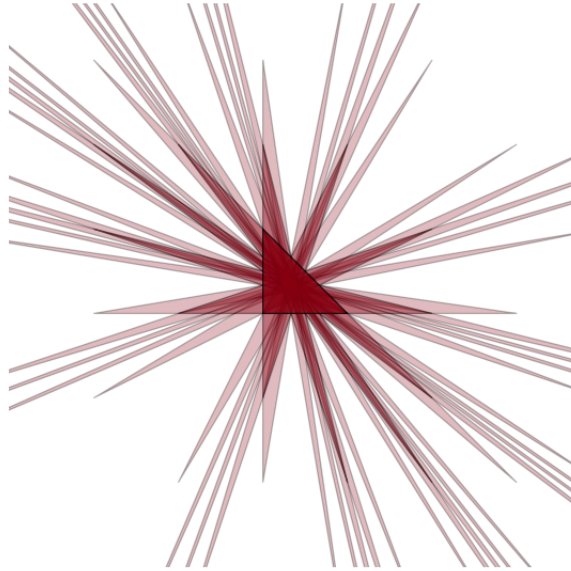


Figure 5.4: The image of the developing map for an almost toric structure on \mathbf{CP}^2 obtained from the standard moment triangle by nodal trades in all three corners.

5.2.2 Remark on monodromy

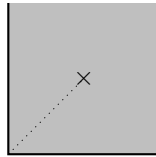
Recall from Remark 4.5.4 that the diagram below has affine monodromy $\begin{pmatrix} 1 & -1 \\ 0 & 1 \end{pmatrix}$ as we go anticlockwise around the branch cut

in order for the broken line to be “straight” in the integral affine structure.



Suppose that we have a nodal trade related to this one by an integral affine transformation A ; then its affine monodromy is $A \begin{pmatrix} 1 & -1 \\ 0 & 1 \end{pmatrix} A^{-1}$.

Example 5.2.3. Consider this diagram:



This is related to the previous one by the matrix $A = \begin{pmatrix} 0 & 1 \\ -1 & -1 \end{pmatrix}$, so the affine monodromy is $\begin{pmatrix} 2 & -1 \\ 1 & 0 \end{pmatrix}$.

More generally, if the eigenray points in the direction $\begin{pmatrix} p \\ q \end{pmatrix}$ then the matrix $\begin{pmatrix} 1 + pq & -p^2 \\ q^2 & 1 - pq \end{pmatrix}$ (or its inverse) is the affine monodromy.

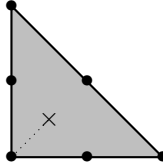
5.2.3 Mutation

When finding a fundamental action domain, we have the freedom to choose a fundamental domain for the action of the deck group on the universal cover. Often, we choose a fundamental domain by making a branch cut from a base node out in the eigendirection of its affine monodromy. If v is an eigenvector then there are two choices: a ray

in the positive v -direction and a ray in the negative v -direction. We can switch between the two by rotating the branch cut through 180 degrees, as we did in Figure 4.5; this operation is called a *mutation* (in fact, in that figure, we rotated by 360 degrees, performing *two mutations*).

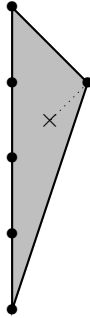
Under a mutation, the fundamental action domain transforms in the following way: it is sliced in two by the eigenray, and the affine monodromy (or its inverse²) is applied to one of the two pieces.

Example 5.2.4. Take a Lagrangian torus fibration on \mathbf{CP}^2 (obtained by a nodal trade from the moment triangle) whose fundamental action domain is as shown in the following picture.

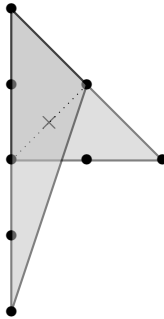


The affine monodromy is $\begin{pmatrix} 2 & -1 \\ 1 & 0 \end{pmatrix}$ as we go anticlockwise around the base node. If we perform a mutation, rotating the branch cut anticlockwise through 180 degrees, then the result is:

²Assume that the affine monodromy is M as we move anticlockwise around the base node. Then, if we are rotating the branch cut anticlockwise then we apply M , while if we are rotating clockwise then we apply M^{-1} .



We superimpose the two pictures for easier comparison.



5.2.4 Nodal slide

Note that there is a free parameter $c > 0$ in the Auroux system. As this parameter varies, we obtain a family of Lagrangian torus fibrations in which the focus-focus singularity moves in the direction of the eigenvector for its affine monodromy (see Figure 5.5). Such a family of fibrations is called a *nodal slide*.

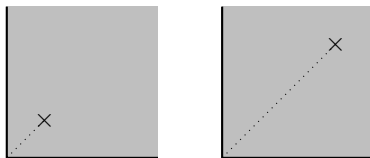


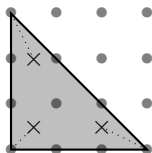
Figure 5.5: A nodal slide.

5.3 Examples

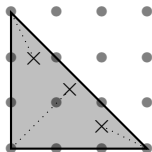
5.3.1 \mathbf{CP}^2 and Markov triples

By combining mutations and nodal trades, we can construct infinitely many inequivalent Lagrangian torus fibrations on the same manifold. The simplest example of this is \mathbf{CP}^2 , where the construction was exploited by Vianna [?] to construct infinitely many distinct Hamiltonian isotopy classes of monotone Lagrangian tori.

Start with the moment triangle and make three nodal trades:

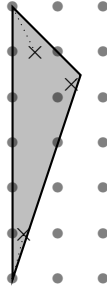


Pick one of the nodes, and slide it towards the opposite edge.



Once it has gone beyond the barycentre of the triangle, perform a

mutation.



Now one can repeat this process *ad infinitum*, picking a different node each time.

To see that you get a different torus fibration in the example above, you can argue as follows. In the first picture, take the eigenray from the lower right node pointing towards the left edge. There is a visible Lagrangian \mathbf{RP}^2 over this ray whose centre is at the focus-focus singularity and meets the toric boundary along the core circle of a Möbius strip. In the final picture, this node has moved to the bottom left, and the same eigenray now points towards the top right edge; the visible Lagrangian is no longer an \mathbf{RP}^2 , as the visible Lagrangian Möbius strip has been replaced by a visible Lagrangian $(5, 1)$ -pinwheel core. This difference in topology distinguishes the torus fibrations.

Remark 5.3.1. It is important to remember that it is the nodal slide which is changing the torus fibration, not the mutation (which only changes the way it is represented).

Remark 5.3.2. Note that all the eigenrays meet at the barycentre of the triangle, which is why we need to nodally slide beyond the barycentre.

Remark 5.3.3. Visible Lagrangians obtained by capping a (p, q) -pinwheel core with a disc are quite common in this context, and

we call them *Lagrangian* (p, q) -*pinwheels*.

Theorem 5.3.4 (Vianna [?, ?]). *The polygons you obtain by iterated mutation and sliding are in bijection with the Markov triples, that is positive integers a, b, c such that $a^2 + b^2 + c^2 = 3abc$. If we write $T(a, b, c)$ for the barycentric fibre of the polygon associated to a, b, c then $T(a, b, c)$ is a monotone Lagrangian torus and the tori associated to distinct Markov triples are not related by a Hamiltonian isotopy.*

Remark 5.3.5. Each polygon looks like a triangle with three nodes, where each node is connected to a vertex by a branch cut. Over the branch cuts we find visible Lagrangian pinwheels $L_{a, q_a}, L_{b, q_b}, L_{c, q_c}$ for some numbers q_a, q_b, q_c . These pinwheels are clearly disjoint from $T(a, b, c)$ as the branch cuts avoid the barycentre. For example $T(1, 1, 2)$ (the *Chekanov torus*) is disjoint from the Lagrangian $L_{2,1} \cong \mathbf{RP}^2$.

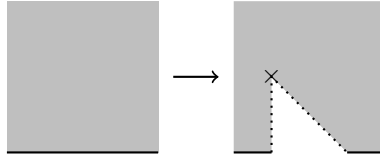
Remark 5.3.6. In all of these Lagrangian torus fibrations, the toric boundary is a symplectic torus in the homology class of a smooth cubic curve. Sikorav [?] has shown that such symplectic tori are all Hamiltonian isotopic to a fixed smooth cubic curve C , so using this Hamiltonian isotopy, we can ensure that the Vianna tori live in the complement of C .

Remark 5.3.7. One can play a similar game with many rational surfaces beyond \mathbf{CP}^2 , see [?].

5.3.2 Blow-up

Theorem 5.3.8. *Let X be a symplectic 4-manifold with a Lagrangian torus fibration $H: X \rightarrow B$. Suppose that $x \in X$ is a point on the toric boundary. Then there is a Lagrangian torus fibration on the symplectic blow-up of X at x ; the fundamental action domain is obtained from the domain before the blow-up by an operation on singular integral affine manifolds affine-isomorphic to that shown in the*

diagram below.

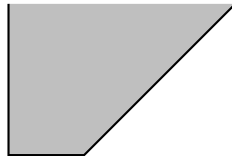


Remark 5.3.9. The observant reader will note that we should specify the size of the symplectic ball we are blowing up. One can read this from the affine geometry: the *affine area* of the triangular segment we are excising will be proportional to the volume of the symplectic ball we are blowing up. By affine area, I mean that the triangular segment is affine-isomorphic to the triangle with vertices at $(0, 0)$, $(1, 0)$, $(0, 1)$, and its affine area is defined to be square of the determinant of the linear part of this affine isomorphism.

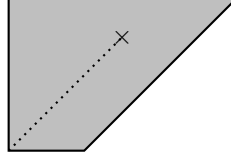
Remark 5.3.10. The affine monodromy is $\begin{pmatrix} 1 & 1 \\ 0 & 1 \end{pmatrix}$, so the image of the toric boundary for the blow-up forms a straight line in the integral affine structure. The toric boundary in the blow-up is the proper transform of the original toric boundary.

Proof. It suffices to find a Lagrangian torus fibration on the holomorphic blow-up of $\mathbf{R} \times S^1 \times \mathbf{C}$ at the point $(0, 1, 0)$ such that the fundamental action domain is the subset shown on the right-hand side of the figure in the statement of the theorem.

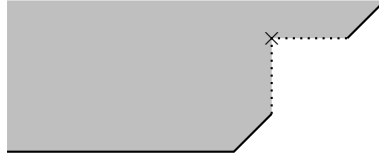
We have seen that $\mathcal{O}(-1)$ is toric with moment polygon:



Make a nodal trade at the bottom left corner and a nodal slide so that if you drop a vertical from the node it hits the slanted edge:



Sweep the branch cut around clockwise until we obtain the following diagram:



If we excise the horizontal part of the toric boundary and apply the affine shear $\begin{pmatrix} 1 & 0 \\ -1 & 1 \end{pmatrix}$ to the diagram then we obtain something which locally resembles the right-hand figure in the statement of the theorem. It remains to show that the space we have just constructed is $Bl_{(0,1,0)}(\mathbf{R} \times S^1 \times \mathbf{C})$.

Note that if we identify $\mathbf{R} \times S^1$ with \mathbf{C}^* then $Bl_{(0,1,0)}(\mathbf{R} \times S^1 \times \mathbf{C})$ can be written as the variety

$$\{(x, y, [a : b]) \in \mathbf{C}^* \times \mathbf{C} \times \mathbf{CP}^1 : ay = b(x - 1)\}.$$

This can be embedded holomorphically into $\mathcal{O}(-1) = \{(z_1, z_2, [a : b]) : az_2 = bz_1\}$ via $(x, y, [a : b]) \mapsto (x+1, y, [a : b])$; the complement of the image of this embedding is the section $\{z_1 = 1\} \subset \mathcal{O}(-1)$. This is the graph of a meromorphic section of $\mathcal{O}(-1)$ with a pole at $[1 : 0]$.

The part of the toric boundary we excised was a symplectic 2-plane which, I claim, is symplectically isotopic to this graph, which completes the proof. To see this, note that the toric boundary before the nodal trade comprised the zero-section and two fibres of the bundle $\mathcal{O}(-1) \rightarrow \mathbf{CP}^1$. When we performed a nodal trade, the new toric boundary became (up to symplectic isotopy) a union of two 2-planes, one isotopic to a fibre and one isotopic to the connected sum of a fibre with the zero-section. If we think of the union of a fibre and the zero-section as the “graph” of a section modelled on a δ -function, then the connected sum of a fibre with the zero-section is the graph of a section with a pole.

□

Remark 5.3.11. We can see a symplectic sphere E with $E^2 = -1$ if we look at the fundamental action domain for the blow-up. It lives over the vertical branch cut, and intersects each torus fibre in an orbit of H_2 (where H_2 is the composition of the action coordinates with the projection to the vertical axis). This is precisely the loop in the torus fibre which collapses at the focus-focus singularity, and which collapses to a point at the toric boundary, so over all we get a sphere. It is easy to check that it is symplectic (to get a visible Lagrangian we would need to take an orbit of H_1 over each point in this line). The fact that it has square -1 is simply because it defines a primitive class in the homology of $\mathcal{O}(-1)$ (for example it has intersection number 1 with the toric boundary considered as a cycle in relative homology) and $H_2(\mathcal{O}(-1); \mathbf{Z})$ is $\mathbf{Z} \cdot E$ where $E^2 = -1$.

Remark 5.3.12. By rotating the branch cut, we obtain another fundamental action domain for this space, shown below.



5.3.3 Rational elliptic surface, K3 surface

Let P, Q be two homogeneous cubic polynomials in three variables and let $\lambda P + \mu Q$ be a family of cubics parametrised by $[\lambda : \mu] \in \mathbf{CP}^1$. This gives a pencil of plane cubic curves:

$$C_{[\lambda:\mu]} = \{[x : y : z] : \lambda P(x, y, z) + \mu Q(x, y, z) = 0\} \subset \mathbf{CP}^2.$$

These curves all intersect at the points $\{[x : y : z] : P(x, y, z) = Q(x, y, z) = 0\}$; this set is called the *base locus* of the pencil. For a generic choice of P, Q , the base locus comprises nine distinct points and there are twelve cubics in the pencil which are singular (having one node each).

If we blow-up the nine basepoints then we get a surface X with a well-defined map $X \rightarrow \mathbf{CP}^1$ whose generic fibres are elliptic curves. This is called a rational elliptic surface (the map is called an elliptic fibration). Figure 5.6 depicts a Lagrangian torus fibration on X , with twelve focus-focus singularities, such that the toric boundary is (symplectically isotopic to) a fibre of the elliptic fibration.

If we take a pair of basis vectors and transport them around a loop very close to the boundary in this fundamental action domain, the total monodromy is trivial. This means that a neighbourhood of the boundary in the integral affine base is isomorphic to a neighbourhood of $S^1 \times \{0\}$ in the integral affine manifold $S^1 \times [0, \infty)$, so the toric boundary of X is a symplectic torus with self-intersection zero.

There is an operation, called *fibre sum* or *Gompf sum*, which, given two symplectic 4-manifolds containing a torus of square zero, produces a new symplectic 4-manifold by cutting out neighbourhoods of these tori and identifying the common boundaries. In our case, the Lagrangian torus fibration clearly extends over the fibre sum; the integral affine base in a neighbourhood of the fibre sum surgery changes from $S^1 \times (-\infty, 0] \cup [0, \infty)$ to $S^1 \times \mathbf{R}$, so the toric boundary disappears after fibre sum. The fibre sum of two rational elliptic surfaces along an elliptic fibre is called a *K3 surface*. We have therefore

constructed a Lagrangian torus fibration on a K3 surface with 24 focus-focus singularities and no toric boundary. The integral affine base is a 2-sphere with 24 base nodes.

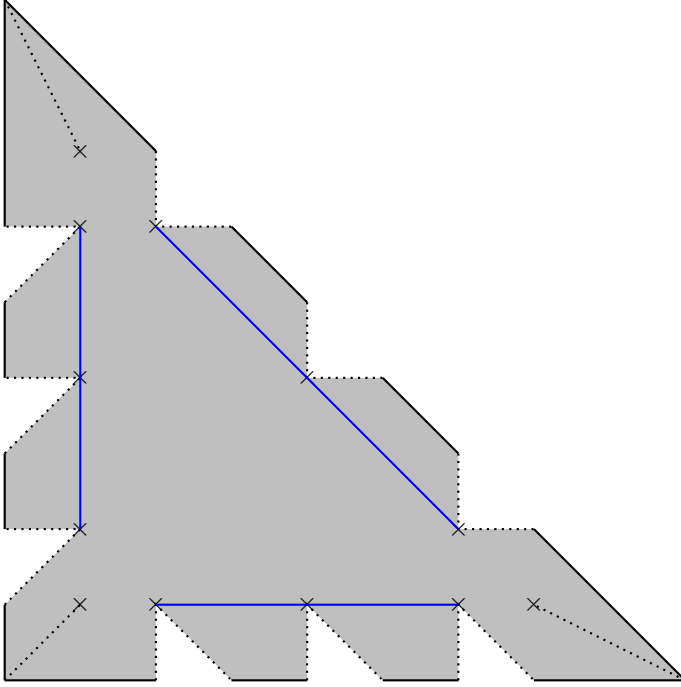
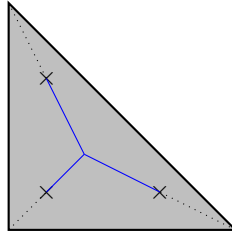


Figure 5.6: A Lagrangian torus fibration on a rational elliptic surface. There are six visible Lagrangian spheres living over the six blue arcs; if we blew up differently-sized balls these spheres would not exist.

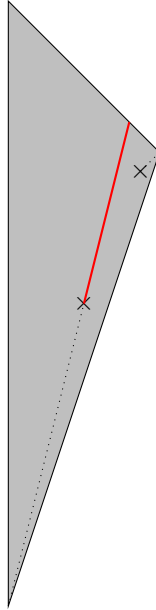
5.4 Exercises



Exercise 5.4.1. Consider the Lagrangian torus fibration on \mathbf{CP}^2 obtained from the standard moment triangle by making three nodal trades (see diagram above, ignoring the blue lines for now). What are the affine monodromies for the three focus-focus singularities? Check that the toric boundary is a straight line closed loop in the affine structure on the base.

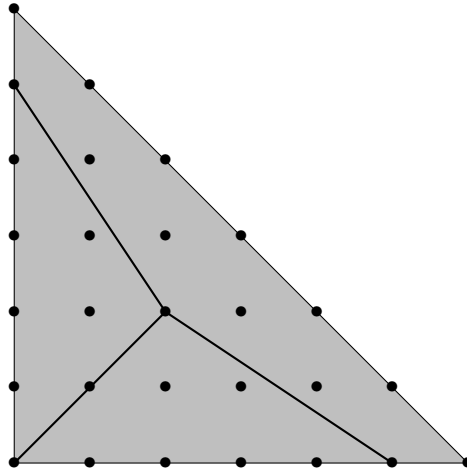
Exercise 5.4.2. The blue lines in the diagram above are visible Lagrangian discs with boundary on the barycentric torus fibre. Sketch the boundaries of these discs in the torus fibre (easiest if you represent the torus as a square with opposite sides identified).

Exercise 5.4.3. The diagram below shows a Lagrangian torus fibration on \mathbf{CP}^2 obtained from the standard moment triangle by two nodal trades and one mutation. Show that the visible Lagrangian over the red line is a Lagrangian pinwheel $L_{5,1}$. Perform another mutation by switching the branch-cut that points in the direction of this red edge and find a Lagrangian $L_{13,2}$ in the result. ****** Prove that \mathbf{CP}^2 contains Lagrangian pinwheels of the form $L_{F_{2n+1}, F_{2n-3}}$ for all n , where $F_1, F_2, F_3, F_4, F_5, F_6, F_7, \dots = 1, 1, 2, 3, 5, 8, 13, \dots$ are the Fibonacci numbers. (More generally, allowing mutations from all three focus-focus singularities, we obtain triples of pairwise disjoint visible Lagrangian pinwheels in bijection with *Markov triples*: triples of positive integers a, b, c satisfying $a^2 + b^2 + c^2 = 3abc$.)

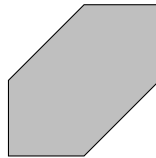


Exercise 5.4.4. Suppose that X has a Lagrangian torus fibration where the singular fibres are only of focus-focus type. Find the Euler characteristic of X . What is the Euler characteristic of a K3 surface?

Exercise 5.4.5. Nemirovski and Shevchishin proved, independently and in very different ways, that there is no embedded Lagrangian Klein bottle in \mathbf{CP}^2 . Why is the following picture not a counterexample to their theorem? ** If it's not an embedded Lagrangian Klein bottle, what is it?



Exercise 5.4.6. Draw some Lagrangian torus fibrations on the 3-point blow-up of \mathbf{CP}^2 by nodal-trading and mutating away from the standard moment hexagon:



Chapter 6

Ruan's construction

In this final lecture, we ask the question: *where do Lagrangian torus fibrations come from?* We have seen that one important source of Lagrangian torus fibrations is toric varieties. We will now present an idea, due to Ruan, which constructs Lagrangian torus fibrations on projective varieties which admit a *toric degeneration*.

6.1 Symplectic parallel transport

Definition 6.1.1 (Degeneration). A *degeneration* is a surjective holomorphic map $\pi: \mathcal{X} \rightarrow S$ where \mathcal{X} is a variety and S is a complex curve. The fibres of the degeneration we will write as $\mathcal{X}_z := \pi^{-1}(z)$ for $z \in S$. A *toric degeneration* is a degeneration in which one of the fibres is a union of (possibly singular) irreducible toric varieties where the union is taken along toric subvarieties.

We tend to think of a degeneration as a family of varieties interpolating between a smooth fibre and another specific (usually singular)

fibre. For those who are versed in the language of algebraic geometry, if π is moreover an algebraic map then it is a flat family of varieties (by [?, III, Proposition 9.7]).

Example 6.1.2. The map $\pi: \mathbf{C}^n \rightarrow \mathbf{C}$, $\pi(z_1, \dots, z_n) = z_1 \cdots z_n$ is a toric degeneration; the singular fibre is $z_1 \cdots z_n = 0$, which is a union of hyperplanes, intersecting along linear subspaces.

Example 6.1.3. Let P, Q are homogeneous polynomials of degree d in $n + 1$ variables, let $\mathcal{X} = \{(z, [\lambda : \mu]) \in \mathbf{CP}^N \times \mathbf{CP}^1 : \lambda P(z) + \mu Q(z) = 0\}$ and consider the projection $\pi: \mathcal{X} \rightarrow \mathbf{CP}^1$. This is a degeneration. If $P(z_1, \dots, z_{n+1}) = z_1 \cdots z_{n+1}$ then it is a toric degeneration (where the specific singular fibre is $\pi^{-1}([1 : 0])$) and the smooth fibres are Calabi-Yau varieties of dimension $n - 1$.

Definition 6.1.4. Suppose we are given a degeneration $\pi: \mathcal{X} \rightarrow S$, a Kähler manifold (Y, ω) and a holomorphic map $F: \mathcal{X} \rightarrow Y$ such that $F|_{\mathcal{X}_z}: \mathcal{X}_z \rightarrow Y$ is an embedding for all $z \in S$. Let $\Omega = F^*\omega$ and write ω_z for the pullback of Ω to \mathcal{X}_z . Although Ω is closed, it could fail to be nondegenerate. However, for each $z \in S$, ω_z is a symplectic form on the smooth locus of \mathcal{X}_z because F is holomorphic. Write \mathcal{V} for the *vertical distribution* on $\mathcal{X} \setminus \text{crit}(\pi)$, that is the distribution with $\mathcal{V}_x = T_x \pi^{-1}(\pi(x))$. A *symplectic connection* on the regular locus of π is a distribution ξ on $\mathcal{X} \setminus \text{crit}(\pi)$ such that:

- ξ is complementary to the vertical distribution, i.e. $T_x \mathcal{X} = \xi_x \oplus \mathcal{V}_x$.
- given a path γ in S which avoids the critical values, the parallel transport map $P: \mathcal{X}_{\gamma(0)} \rightarrow \mathcal{X}_{\gamma(1)}$ satisfies $P^* \omega_{\gamma(1)} = \omega_{\gamma(0)}$.

Lemma 6.1.5. *Suppose we are given a degeneration $\pi: \mathcal{X} \rightarrow S$, a Kähler manifold (Y, ω) and a holomorphic map $F: \mathcal{X} \rightarrow Y$ such that $F|_{\mathcal{X}_z}: \mathcal{X}_z \rightarrow Y$ is an embedding for all $z \in S$. Then there is a canonical symplectic connection, given by*

$$\xi_x = \{v \in T_x \mathcal{X} : \Omega(v, w) = 0 \text{ for all } w \in T_x \pi^{-1}(\pi(x))\}.$$

Proof. First note that ξ_x is complementary to the vertical distribution: since \mathcal{V}_x is symplectic, it has zero intersection with ξ_x , and since ξ_x is isomorphic to the annihilator of \mathcal{V}_x , it is a complement.

To see that the parallel transport map $P_t: \mathcal{X}_{\gamma(0)} \rightarrow \mathcal{X}_{\gamma(t)}$ is symplectic, we need to check that $\Omega((P_t)_*v_1, (P_t)_*v_2)$ is constant in t for any vertical vectors v_1, v_2 . This amounts to checking that the Lie derivative $L_{\tilde{\gamma}(t)}\Omega$ vanishes on pairs of vertical vectors, where $\tilde{\gamma}(t)$ denotes the horizontal lift of the tangent vector $\dot{\gamma}(t)$. Since Ω is closed, Cartan's formula tells us that this Lie derivative is equal to $d\iota_{\tilde{\gamma}(t)}\Omega$. Since $\eta := \iota_{\tilde{\gamma}(t)}\Omega$ vanishes on vertical vectors (by definition of the connection), its differential also vanishes on vertical vectors. To see this, note that the vertical distribution is integrable (with integral submanifolds the fibres!) so

$$d\eta(v_1, v_2) = v_1\eta(v_2) - v_2\eta(v_1) - \eta([v_1, v_2]),$$

which vanishes because η annihilates vertical vectors and $v_1, v_2, [v_1, v_2]$ are all vertical.

□

Example 6.1.6. Consider the variety $\mathcal{X} = \mathbf{C}^{n+1}$ and the map $\pi(z) = \sum_{i=1}^{n+1} z_i^2$. This is a degeneration whose fibres are complex n -dimensional quadrics, precisely one of which is singular, \mathcal{X}_0 . Note that $d\pi(v_1, \dots, v_{n+1}) = 2 \sum_{i=1}^{n+1} x_i v_i$. We use the symplectic form $\Omega = \frac{i}{2} \sum dz_j \wedge d\bar{z}_j$. Since the vertical distribution is annihilated

by $d\pi$, it follows that $\begin{pmatrix} \bar{z}_1 \\ \vdots \\ \bar{z}_{n+1} \end{pmatrix}$ is a horizontal vector field and that

$\frac{v}{2|z|^2} \begin{pmatrix} \bar{z}_1 \\ \vdots \\ \bar{z}_{n+1} \end{pmatrix}$ is a horizontal vector at z which projects (via $d\pi$) to

the vector $v \in \mathbf{C}$. In particular, the vector field

$$\frac{-1}{2|z|^2} \begin{pmatrix} \bar{z}_1 \\ \vdots \\ \bar{z}_{n+1} \end{pmatrix}$$

is a horizontal lift of the vector field which points in the negative real direction in \mathbf{C} . Parallel transport along the path $\gamma(s) = 1 - s$ (from \mathcal{X}_1 to \mathcal{X}_0) can be understood by solving the differential equations

$$\begin{aligned} \dot{z}_1 &= -z_1 \\ &\vdots \\ \dot{z}_{n+1} &= -z_{n+1} \\ \dot{\lambda} &= -2|z|^2 \end{aligned}$$

(where $\lambda(0) = 1$ and $\lambda(t)$ is the projection of $(z_1(t), \dots, z_{n+1}(t))$ at time t). The solution starting from $\lambda(0) = 1$ is

$$\begin{aligned} z_k(t) &= a_k(t) + ib_k(t) \\ \lambda(t) &= 1 + \sum (a_k(0)^2(e^{-2t} - 1) - b_k(0)^2(e^{2t} - 1)) \end{aligned}$$

where $a_k(t) = a_k(0)e^{-t}$ and $b_k(t) = b_k(0)e^t$. The real part of the quadric therefore converges to the singular point $0 \in \mathcal{X}_0$ as $t \rightarrow \infty$, while $\lambda(t) \rightarrow 0$ for points on the real locus in \mathcal{X}_1 . The real part of the quadric is an n -sphere, which we call the *vanishing cycle* of the degeneration.

6.2 Lagrangian torus fibrations

Suppose we are given a degeneration $\pi: \mathcal{X} \rightarrow S$, two points $0, z \in S$ such that \mathcal{X}_0 is a singular fibre and \mathcal{X}_z is smooth, and a path γ from z to 0 which avoids the critical values except $\gamma(1) = 0$. A

priori, the parallel transport map $P: \mathcal{X}_z \rightarrow \mathcal{X}_0$ is only well-defined away from some subset of \mathcal{X}_z , but if we understand the local model for π near \mathcal{X}_0 well enough then we can extend P continuously to the whole of \mathcal{X}_z . For example, if \mathcal{X}_0 has an ordinary double point then the local model from Example 6.1.6 tells us that, although the parallel transport map is not defined along the vanishing cycle, we can extend it continuously by sending all the points in the vanishing cycle to the singularity.

Ruan’s idea for constructing Lagrangian torus fibrations is to take a toric degeneration (where \mathcal{X}_0 is a union of toric varieties glued along toric strata) and compose the parallel transport map P with the moment maps for \mathcal{X}_0 . The main technical difficulties in this approach arise from trying to understand the local models for what vanishes in such toric degenerations.

We will start by examining the simplest local model of all, namely Example 6.1.2, where the total space is smooth and \mathcal{X}_0 has normal crossing singularities. We begin with a lemma.

Lemma 6.2.1. *Suppose that H is a Hamiltonian function on (\mathcal{X}, Ω) and suppose that H has Hamiltonian flow ϕ_t^H and that $\pi(\phi_t^H(x)) = \pi(x)$ for all $x \in \mathcal{X}$, $t \in \mathbf{R}$ then H is preserved by symplectic parallel transport, that is*

$$H(P_t(x)) = H(x)$$

for all $x \in \mathcal{X}$, $t \in \mathbf{R}$, where P_t is the time- t parallel transport symplectomorphism along γ .

Remark 6.2.2. We are not assuming that Ω is symplectic, only closed, so it is not immediate that the Hamiltonian vector field v_H exists. Hence the wording “suppose that H has a Hamiltonian flow” in the statement of the lemma.

Proof of Lemma 6.2.1. Let $\tilde{\gamma}(t)$ be the horizontal lift of $\dot{\gamma}(t)$. We want to show that

$$L_{\tilde{\gamma}(t)}H = 0.$$

We have

$$L_{\tilde{\gamma}(t)}H = i_{\tilde{\gamma}(t)}dH = -\Omega(v, \tilde{\gamma}(t)).$$

Differentiating $\pi(\phi_t^H(x)) = \pi(x)$ with respect to t , we get $\pi_*v = 0$, so v is tangent to the fibres of π . Therefore v is Ω -orthogonal to the horizontal distribution, so $\Omega(v, \tilde{\gamma}(t)) = 0$, as required.

□

Theorem 6.2.3. *Let $\mathcal{X} = \mathbf{C}^{n+1}$ and let $\pi: \mathcal{X} \rightarrow \mathbf{C}$ be the map $\pi(z_0, \dots, z_n) = z_0 \cdots z_n$. Let $P_t: \mathcal{X}_1 \rightarrow \mathcal{X}_{1-t}$ be the parallel transport map for the symplectic connection associated to the standard symplectic form Ω on \mathbf{C}^{n+1} . Let $\mu: \mathcal{X}_0 \rightarrow \mathbf{R}^n$ be the moment map $\mu(z_0, z_1, \dots, z_n) = (\frac{1}{2}(|z_1|^2 - |z_0|^2), \dots, \frac{1}{2}(|z_n|^2 - |z_0|^2))$ which restricts to a moment map for the standard T^n -action on each irreducible component of \mathcal{X}_0 . Then the composition $\mu \circ P$ is a smooth Lagrangian torus fibration with no singular fibres on \mathcal{X}_1 . Indeed, if we identify $\mathcal{X}_1 = \left\{ (z_0, \dots, z_n) : z_0 = \frac{1}{z_1 \cdots z_n} \right\}$ with $(\mathbf{C}^*)^n$ then the fibres of $\mu \circ P$ are precisely the product tori $S_{r_1}^1 \times \cdots \times S_{r_n}^1 \subset (\mathbf{C}^*)^n$ where $S_r^1 \subset \mathbf{C}^*$ denotes a circle of radius r centred at 0.*

Proof. The map μ is the restriction to \mathcal{X}_0 of the map $\mu: \mathcal{X} \rightarrow \mathbf{R}^n$ defined by the same formula. The restriction of μ to \mathcal{X}_1 gives the Lagrangian torus fibration $|z_k|^2 - \frac{1}{|z_1 \cdots z_n|^2} = 2\mu_k$, $k = 1, \dots, n$, which is precisely a system of simultaneous equations fixing the radii $|z_k|$ in terms of the numbers μ_k . Therefore it suffices to show that $\mu(P(x)) = \mu(x)$. This follows from Lemma 6.2.1 because each component μ_k generates a Hamiltonian circle action on \mathcal{X} given by $(e^{-it}z_0, z_1, \dots, z_{k-1}, e^{it}z_k, z_{k+1}, \dots, z_n)$, which preserves the fibres of π .

□

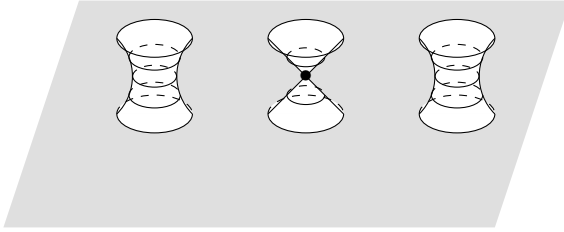


Figure 6.1: The parallel transport for the fibration $(z_0, z_1) \mapsto z_0 z_1$ preserves the level sets of the function $\mu_1 = \frac{1}{2} (|z_1|^2 - |z_0|^2)$.

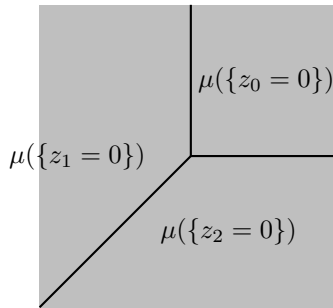
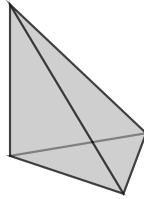


Figure 6.2: The image of $\mu: \mathcal{X}_0 \rightarrow \mathbf{R}^n$ for the case $n = 2$.

6.3 Quartic pencil

We now try a more ambitious construction. Consider the variety $\mathcal{X} = \{([x, y, z, w], \lambda) \in \mathbf{CP}^3 \times \mathbf{C} : xyzw + \lambda(x^4 + y^4 + z^4 + w^4) = 0\}$ and the map $\pi: \mathcal{X} \rightarrow \mathbf{C}$, $\pi([x, y, z, w], \lambda) = \lambda$, where the smooth fibre \mathcal{X}_1 is a quartic (K3) surface and the singular fibre \mathcal{X}_0 is a union of four copies of \mathbf{CP}^2 in a “tetrahedron” configuration, like you find at the toric boundary for the standard torus action on \mathbf{CP}^3 :



We wish to use Ruan's idea to construct a Lagrangian torus fibration on the smooth K3 surface, but we know that we need to introduce 24 focus-focus singularities to achieve that, and in Theorem 6.2.3 we did not introduce any singular fibres. Nonetheless, \mathcal{X}_0 is a normal crossing variety (i.e. locally modelled on the singular fibre in Theorem 6.2.3. What is going on?

Although \mathcal{X}_0 is normal crossing, the total space \mathcal{X} has singularities in the locus $\lambda = 0$. Indeed, the singularities lie at the points where

$$\begin{aligned}
 0 &= xyzw + \lambda(x^4 + y^4 + z^4 + w^4) \\
 0 &= \frac{\partial}{\partial \lambda} (xyzw + \lambda(x^4 + y^4 + z^4 + w^4)) \\
 &= x^4 + y^4 + z^4 + w^4, \\
 0 &= \frac{\partial}{\partial x} (xyzw + \lambda(x^4 + y^4 + z^4 + w^4)) \\
 &= yzw + 4\lambda x^3 \\
 &\vdots \\
 0 &= \frac{\partial}{\partial w} (xyzw + \lambda(x^4 + y^4 + z^4 + w^4)) \\
 &= xyz + 4\lambda w^3.
 \end{aligned}$$

The first two equations imply $xyzw = 0$ so at least one of x, y, z, w must vanish. The final four equations imply that if one of x, y, z, w vanish then $\lambda = 0$ and actually *two* of x, y, z, w must vanish. This implies that the singular locus of \mathcal{X} is contained in $\lambda = 0$ and is the intersection of $x^4 + y^4 + z^4 + w^4 = 0$ with the six lines $x = y = 0$,

$x = z = 0$, $x = w = 0$, $y = z = 0$, $y = w = 0$, $z = w = 0$. This is precisely 24 points, four on each of the six lines.

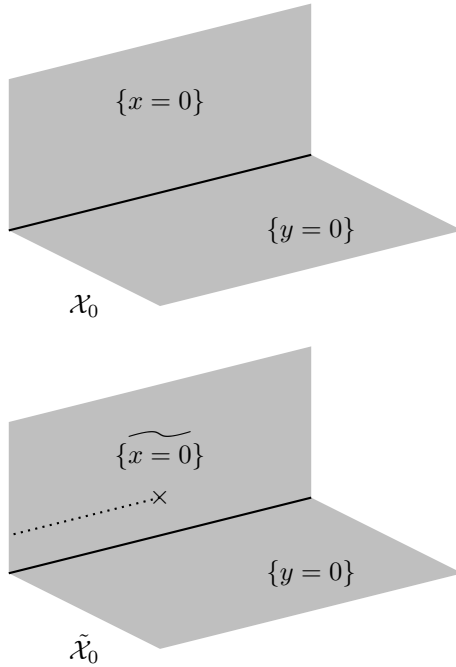
The singularities of \mathcal{X} are ordinary double point singularities, so we need to analyse the local model for a degeneration of surfaces when the total space has an ordinary double point.

Example 6.3.1. Consider the space $\mathcal{X} = \{(x, y, z, \lambda) \in \mathbf{C}^2 \times \mathbf{C}^* \times \mathbf{C} : xy = \lambda(z-1)\}$. This has an ordinary double point at $(0, 0, 1, 0)$. The projection $\pi: \mathcal{X} \rightarrow \mathbf{C}$, $\pi(x, y, z, \lambda) = \lambda$, is a degeneration which gives a local model for the quartic pencil we are considering. The smooth fibre $xy = z - 1$, $z \in \mathbf{C}^*$, has a Lagrangian torus fibration with a focus-focus singularity $(\frac{1}{2}(|x|^2 - |y|^2), \frac{1}{2}|xy + 1|^2)$ which is essentially the Auroux system minus its toric boundary.

Here is how we can reconstruct this fibration using Ruan's idea. When $\lambda = 0$, the fibre \mathcal{X}_0 is the space $\{x = 0\} \cup \{y = 0\}$, which is a union of two copies of $\mathbf{C} \times \mathbf{C}^*$ along a \mathbf{C}^* . We birationally modify \mathcal{X} by making a *small resolution* at the ordinary double point. In other words, we consider the space

$$\tilde{\mathcal{X}} := \{(x, y, z, \lambda, [a : b]) : ax = b\lambda, a(z - 1) = by\},$$

in which the preimage of the singular point $(0, 0, 1, 0)$ under the projection to (x, y, z, λ) is the sphere $\{(0, 0, 1, 0)\} \times \mathbf{CP}^1$. We get a new degeneration $\tilde{\pi}: \tilde{\mathcal{X}} \rightarrow \mathbf{C}$ whose fibre $\tilde{\mathcal{X}}_z$ over z is the proper transform of \mathcal{X}_z . Since the small resolution only affects the fibre \mathcal{X}_0 , we need to find the proper transform of $\mathcal{X}_0 = \{x = 0\} \cup \{y = 0\}$. The proper transform of the subvariety $\{x = 0\}$ is $\{(0, y, z, 0, [a : b]) : a(z - 1) = by\}$, which is isomorphic to $Bl_{(0,1)}(\mathbf{C}_y \times \mathbf{C}_z^*)$. The proper transform of the subvariety $\{y = 0\}$ is the subvariety $\{(x, 0, z, [0 : 1])\}$, which is isomorphic to $\mathbf{C}^* \times \mathbf{C}$. Overall, $\tilde{\mathcal{X}}_0$ admits a Lagrangian torus fibration, which is given by Theorem 5.3.8 (Remark 5.3.12) on the proper transform of $\{x = 0\}$, and which is toric on the proper transform of $\{y = 0\}$. This has one focus-focus singularity, and a line of toric singularities which disappear once we pass to the smooth fibre because these singularities are handled by Theorem 6.2.3.

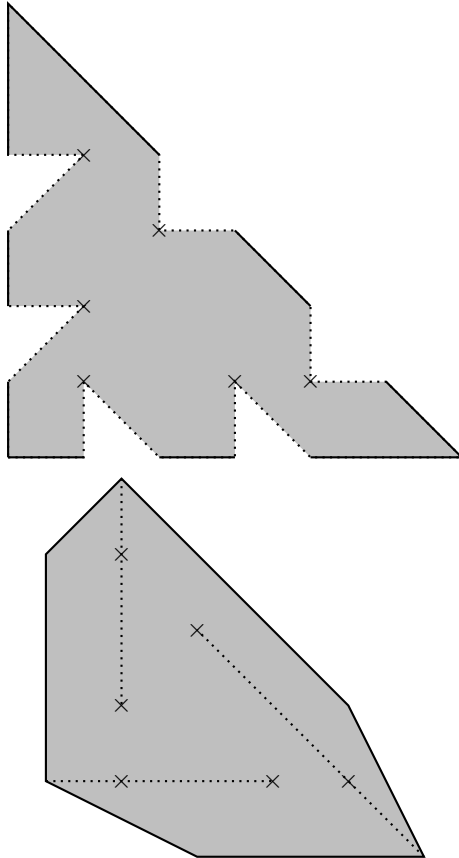


Remark 6.3.2. There is a choice when making the small resolution: the variety

$$\tilde{\mathcal{X}}' := \{(x, y, z, \lambda, [a : b]) : ay = b\lambda, a(z - 1) = bx\}$$

would do just as well, and would result in the other irreducible component of \mathcal{X}_0 being blown-up.

Finally, returning to the quartic pencil, we make a small resolution at each of the 24 singular points. This involves 24 choices, and we make the most symmetric possible, in which each plane in our tetrahedron gets blown-up six times (twice on each edge). Here are two pictures (related by changes of branch cuts) which show what each plane looks like after this modification:



A Lagrangian torus fibration is obtained on the smoothing the union of these blown-up planes using Theorem 6.2.3 (which is applicable now as the total space is now smooth). The result is a Lagrangian torus fibration over the sphere with 24 focus-focus singularities.

Remark 6.3.3. It is a theorem of Mumford that any degeneration can be modified (by possibly pulling back along a branched cover of the base and making birational modifications to the total space) so that

the total space is smooth and the singular fibre is a reduced normal crossing variety. The local model from Theorem 6.2.3 applies in this case provided we can find suitable Lagrangian torus fibrations on the irreducible components.

6.4 Exercises

Exercise 6.4.1. Consider the degeneration $\pi: \mathbf{C}^2 \rightarrow \mathbf{C}$, $\pi(z_1, z_2) = z_1 z_2$, and let $\Omega = dx_1 \wedge dy_1 + dx_2 \wedge dy_2$ (with $z_k = x_k + iy_k$). Check that the horizontal lift (for the canonical symplectic connection) of the vector $v \in \mathbf{C}$ at (z_1, z_2) is $\tilde{v} = \frac{v}{|z|^2} \begin{pmatrix} \bar{z}_2 \\ \bar{z}_1 \end{pmatrix}$ where $|z|^2 = |z_1|^2 + |z_2|^2$. Let $\gamma(t) = e^{2\pi it}$ be a parametrisation of the unit circle in \mathbf{C} and write $z_1(t) = r(t)e^{i\theta(t)}$, $z_2(t) = e^{2\pi it - \theta(t)}/r$ for the path traced out by $(z_1(0), z_2(0))$ under symplectic parallel transport. Show that $\dot{r} = 0$ and $\dot{\theta} = \frac{1}{r^4 + 1}$. Hence find the parallel transport at time 1. Plot the image of the line $\theta = 0$ under the parallel transport map. You just showed that the time 1 parallel transport is a *Dehn twist*.

Exercise 6.4.2. Show that the map $H: \mathbf{C}^3 \rightarrow \mathbf{R}^3$, $H(x, y, z) = (\frac{1}{2}(|x|^2 - |y|^2), \frac{1}{2}(|x|^2 - |z|^2), \frac{1}{2}|xyz - c|)$ is a Lagrangian torus fibration. What are the singular fibres? Show that the set of singular fibres forms a Y-graph in \mathbf{R}^3 .

Bibliography

- [1] V. I. Arnol'd. *Mathematical methods of classical mechanics*, volume 60 of *Graduate Texts in Mathematics*. Springer-Verlag, New York, 1989. Translated from the 1974 Russian original by K. Vogtmann and A. Weinstein, second edition.
- [2] D. Auroux. Mirror symmetry and T -duality in the complement of an anticanonical divisor. *J. Gökova Geom. Topol. GGT*, 1:51–91, 2007.
- [3] M. Chaperon. Normalisation of the smooth focus-focus: a simple proof. *Acta Math. Vietnam.*, 38(1):3–9, 2013.
- [4] J.-P. Dufour and P. Molino. Compactification d'actions de \mathbf{R}^n et variables action-angle avec singularités. In *Travaux du Séminaire Sud-Rhodanien de Géométrie, I*, volume 88 of *Publ. Dép. Math. Nouvelle Sér. B*, pages 161–183. Univ. Claude-Bernard, Lyon, 1988.
- [5] J. J. Duistermaat. On global action-angle coordinates. *Comm. Pure Appl. Math.*, 33(6):687–706, 1980.
- [6] L. H. Eliasson. Normal forms for Hamiltonian systems with Poisson commuting integrals—elliptic case. *Comment. Math. Helv.*, 65(1):4–35, 1990.

- [7] J. Kollár and N. I. Shepherd-Barron. Threefolds and deformations of surface singularities. *Invent. Math.*, 91(2):299–338, 1988.
- [8] R. Schoen and J. Wolfson. Minimizing area among Lagrangian surfaces: the mapping problem. *J. Differential Geom.*, 58(1):1–86, 2001.
- [9] D. Sepe and S. Vũ Ngọc. Integrable systems, symmetries, and quantization. *Lett. Math. Phys.*, 108(3):499–571, 2018.
- [10] M. Symington. Four dimensions from two in symplectic topology. In *Topology and geometry of manifolds (Athens, GA, 2001)*, volume 71 of *Proc. Sympos. Pure Math.*, pages 153–208. Amer. Math. Soc., Providence, RI, 2003.
- [11] S. Vũ Ngọc. On semi-global invariants for focus-focus singularities. *Topology*, 42(2):365–380, 2003.